Cell Host & Microbe, Volume *20*

Supplemental Information

Identification of Interferon-Stimulated Genes with Antiretroviral Activity

Melissa Kane, Trinity M. Zang, Suzannah J. Rihn, Fengwen Zhang, Tonya Kueck, Mudathir Alim, John Schoggins, Charles M. Rice, Sam J. Wilson, and Paul D. Bieniasz

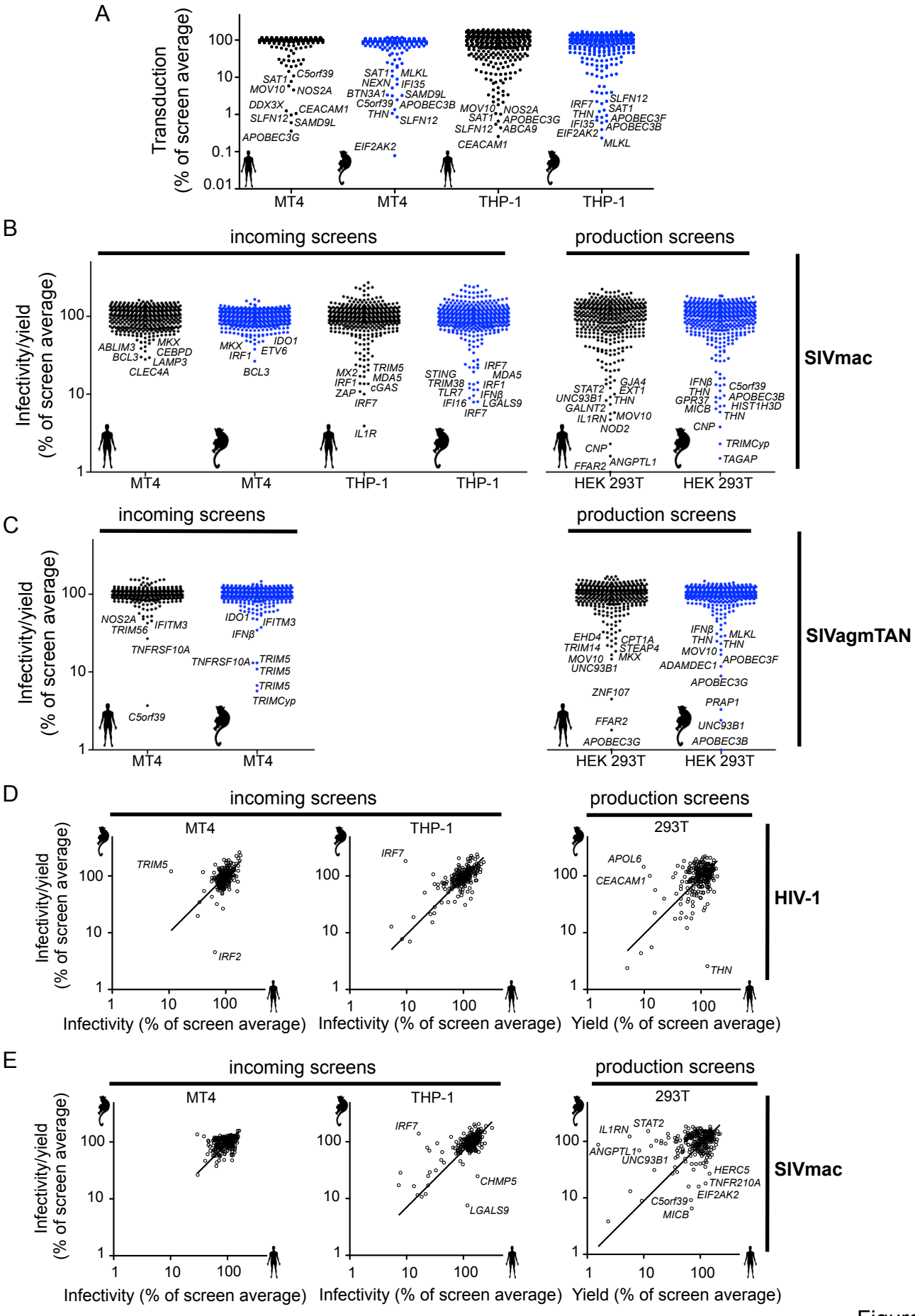
A
Transduction (% of screen average)
100
10
1
0.1
0.01
SAT1
C5orf39
MOV10
NOS2A
DDX3X
CEACAM1
SLFN12
SAMD9L
APOBEC3G
SAT1
MLKL
NEXN
IFI35
BTN3A1
SAMD9L
C5orf39
APOBEC3B
THN
SLFN12
EIF2AK2
MOV10
NOS2A
SAT1
APOBEC3G
SLFN12
ABCA9
CEACAM1
IRF7
SLFN12
THN
SAT1
IFI35
APOBEC3F
EIF2AK2
APOBEC3B
MLKL
MT4
MT4
THP-1
THP-1
B
incoming screens
production screens
Infectivity/yield (% of screen average)
100
10
1
ABLIM3
MKX
BCL3
CEBPD
LAMP3
CLEC4A
MKX
IDO1
IRF1
ETV6
BCL3
MX2
TRIM5
IRF1
MDA5
ZAP
cGAS
IRF7
IL1R
STING
IRF7
TRIM38
MDA5
TLR7
IRF1
IFI16
IFNβ
LGALS9
IRF7
STAT2
GJA4
UNC93B1
EXT1
GALNT2
THN
IL1RN
MOV10
NOD2
CNP
FFAR2
ANGPTL1
IFNβ
C5orf39
THN
APOBEC3B
GPR37
HIST1H3D
MICB
THN
CNP
TRIMCyp
TAGAP
MT4
MT4
THP-1
THP-1
HEK 293T
HEK 293T
SIVmac
C
incoming screens
production screens
Infectivity/yield (% of screen average)
100
10
1
NOS2A
IFITM3
TRIM56
TNFRSF10A
IDO1
IFITM3
IFNβ
TNFRSF10A
TRIM5
TRIM5
TRIM5
TRIMCyp
C5orf39
EHD4
CPT1A
TRIM14
STEAP4
MOV10
MKX
UNC93B1
ZNF107
FFAR2
APOBEC3G
IFNβ
MLKL
THN
THN
MOV10
APOBEC3F
ADAMDEC1
APOBEC3G
PRAP1
UNC93B1
APOBEC3B
MT4
MT4
HEK 293T
HEK 293T
SIVagmTAN
D
incoming screens
production screens
MT4
THP-1
293T
Infectivity/yield (% of screen average)
100
10
1
TRIM5
IRF2
IRF7
APOL6
CEACAM1
THN
1
10
100
Infectivity (% of screen average)
Infectivity (% of screen average)
Yield (% of screen average)
HIV-1
E
incoming screens
production screens
MT4
THP-1
293T
Infectivity/yield (% of screen average)
100
10
1
IRF7
CHMP5
LGALS9
IL1RN
STAT2
ANGPTL1
UNC93B1
HERC5
TNFR210A
EIF2AK2
C5orf39
MICB
1
10
100
Infectivity (% of screen average)
Infectivity (% of screen average)
Yield (% of screen average)
SIVmac

Figure S1

Fig S1. Effects of human and macaque ISGs on vector production and primate lentiviruses (Related to Figure 1).

(A) Effects of ISG encoding vectors on vector transduction in MT4 and THP-1 cells.

(B, C) Effects of ISGs in incoming screens with SIVmac (B) in MT4 and THP-1 cells; and SIVagmTAN, (C) in MT4 cells only, and effects of the same ISGs on the generation of infectious SIVmac (B) and SIVagmTAN (C) particles in 293T cells.

(D, E) Comparison of the effects of human and macaque ISGs (genes in both libraries) in incoming screens with HIV-1 (D) and SIVmac (E) in MT4 and THP-1 cells, and effects of the same ISGs on the generation of infectious HIV-1 (D) and SIVmac (E) from 293T cells. All screens were normalised to the screen average (100 arbitrary units).

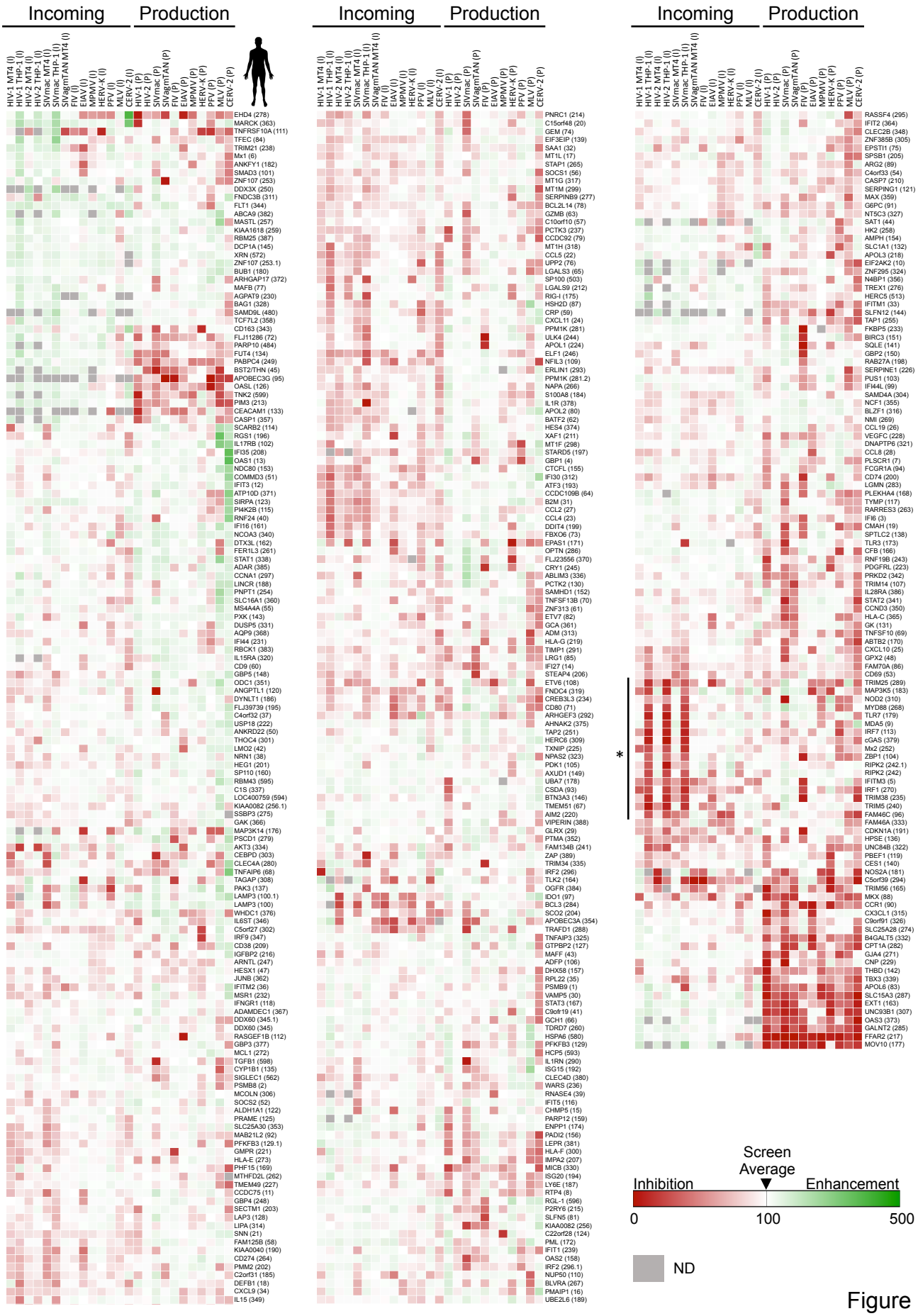
Incoming
Production
HIV-1 MT4 (I)
HIV-1 THP-1 (I)
HIV-2 MT4 (I)
HIV-2 THP-1 (I)
SIVmac MT4 (I)
SIVmac THP-1 (I)
SIVagmTAN MT4 (I)
FIV (I)
EIAV (I)
MPMV (I)
HERV-K (I)
PFV (I)
MLV (I)
CERV-2 (I)
HIV-1 (P)
HIV-2 (P)
SIVmac (P)
SIVagmTAN (P)
FIV (P)
EIAV (P)
MPMV (P)
HERV-K (P)
PFV (P)
MLV (P)
CERV-2 (P)
EHD4 (278)
MARCK (363)
TNFRSF10A (111)
TFEC (84)
TRIM21 (238)
Mx1 (6)
ANKFY1 (182)
SMAD3 (101)
ZNF107 (253)
DDX3X (250)
FNDC3B (311)
FLT1 (344)
ABCA9 (382)
MASTL (257)
KIAA1618 (259)
RBM25 (387)
DCP1A (145)
XRN (572)
ZNF107 (253.1)
BUB1 (180)
ARHGAP17 (372)
MAFB (77)
AGPAT9 (230)
BAG1 (328)
SAMD9L (480)
TCF7L2 (358)
CD163 (343)
FLJ11286 (72)
PARP10 (484)
FUT4 (134)
PABPC4 (249)
BST2/THN (45)
APOBEC3G (95)
OASL (126)
TNK2 (599)
PIM3 (213)
CEACAM1 (133)
CASP1 (357)
SCARB2 (114)
RGS1 (196)
IL17RB (102)
IFI35 (208)
OAS1 (13)
NDC80 (153)
COMMD3 (51)
IFIT3 (12)
ATP10D (371)
SIRPA (123)
PI4K2B (115)
RNF24 (40)
IFI16 (161)
NCOA3 (340)
DTX3L (162)
FER1L3 (261)
STAT1 (338)
ADAR (385)
CCNA1 (297)
LINCR (188)
PNPT1 (254)
SLC16A1 (360)
MS4A4A (55)
PXK (143)
DUSP5 (331)
AQP9 (368)
IFI44 (231)
RBCK1 (383)
IL15RA (320)
CD9 (60)
GBP5 (148)
ODC1 (351)
ANGPTL1 (120)
DYNLT1 (186)
FLJ39739 (195)
C4orf32 (37)
USP18 (222)
ANKRD22 (50)
THOC4 (301)
LMO2 (42)
NRN1 (38)
HEG1 (201)
SP110 (160)
RBM43 (595)
C1S (337)
LOC400759 (594)
KIAA0082 (256.1)
SSBP3 (275)
GAK (366)
MAP3K14 (176)
PSCD1 (279)
AKT3 (334)
CEBPD (303)
CLEC4A (280)
TNFAIP6 (68)
TAGAP (308)
PAK3 (137)
LAMP3 (100.1)
LAMP3 (100)
WHDC1 (376)
IL6ST (346)
C5orf27 (302)
IRF9 (347)
CD38 (209)
IGFBP2 (216)
ARNTL (247)
HESX1 (47)
JUNB (362)
IFITM2 (36)
MSR1 (232)
IFNGR1 (118)
ADAMDEC1 (367)
DDX60 (345.1)
DDX60 (345)
RASGEF1B (112)
GBP3 (377)
MCL1 (272)
TGFB1 (598)
CYP1B1 (135)
SIGLEC1 (562)
PSMB8 (2)
MCOLN (306)
SOCS2 (52)
ALDH1A1 (122)
PRAME (125)
SLC25A30 (353)
MAB21L2 (92)
PFKFB3 (129.1)
GMPR (221)
HLA-E (273)
PHF15 (169)
MTHFD2L (262)
TMEM49 (227)
CCDC75 (11)
GBP4 (248)
SECTM1 (203)
LAP3 (128)
LIPA (314)
SNN (21)
FAM125B (58)
KIAA0040 (190)
CD274 (264)
PMM2 (202)
C2orf31 (185)
DEFB1 (18)
CXCL9 (34)
IL15 (349)
PNRC1 (214)
C15orf48 (20)
GEM (74)
EIF3EIP (139)
SAA1 (32)
MT1L (17)
STAP1 (265)
SOCS1 (56)
MT1G (317)
MT1M (299)
SERPINB9 (277)
BCL2L14 (78)
GZMB (63)
C10orf10 (57)
PCTK3 (237)
CCDC92 (79)
MTTH (318)
CCL5 (22)
UPP2 (76)
LGALS3 (65)
SP100 (503)
LGALS9 (212)
RNASE6 (175)
HSH2D (87)
CRP (59)
CXCL11 (24)
PPM1K (281)
ULK4 (244)
APOL1 (224)
ELF1 (246)
NFIL3 (109)
ERLIN1 (293)
PPM1K (281.2)
NAPA (266)
S100A8 (184)
IL1R (378)
APOL2 (80)
BATF2 (62)
HES4 (374)
XAF1 (211)
MT1F (298)
STARD5 (197)
GBP1 (4)
CTCFL (155)
IFI30 (312)
ATF3 (193)
CCDC109B (64)
B2M (31)
CCL2 (27)
CCL4 (23)
DDIT4 (199)
FBXO6 (73)
EPAS1 (171)
OPTN (286)
FLJ23556 (370)
CRY1 (245)
ABLIM3 (336)
PCTK2 (130)
SAMHD1 (152)
TNFSF13B (70)
ZNF313 (61)
ETV7 (82)
GCA (361)
ADM (313)
HLA-G (219)
TIMP1 (291)
LRG1 (85)
IFI27 (14)
STEAP4 (206)
ETV6 (108)
FNDC4 (319)
CREB3L3 (234)
CD80 (71)
ARHGEF3 (292)
AHNAK2 (375)
TAP2 (251)
HERC6 (309)
TXNIP (225)
NPAS2 (323)
PDK1 (105)
AXUD1 (149)
UBA7 (178)
CSDA (93)
BTN3A3 (146)
TMEM51 (67)
AIM2 (220)
VIPERIN (388)
GLRX (29)
PTMA (352)
FAM134B (241)
ZAP (389)
TRIM34 (335)
IRF7 (296)
TLK2 (164)
OGFR (384)
IDO1 (97)
BCL3 (284)
SCO2 (204)
APOBEC3A (354)
TRAFD1 (288)
TNFAIP3 (325)
GTPBP2 (127)
MAFF (43)
ADFP (106)
HERC5 (157)
RPL22 (35)
PSMB9 (1)
VAMP5 (30)
STAT3 (167)
C9orf19 (41)
GCH1 (66)
TDRD7 (260)
HSPA6 (580)
PFKFB3 (129)
HCP5 (593)
IL1RN (290)
ISG15 (192)
CLEC4D (380)
WARS (236)
RNASE4 (39)
IFIT5 (116)
CH25H (15)
PARP12 (159)
ENPP1 (174)
PADI2 (156)
LEPR (381)
HLA-F (300)
IMPA2 (207)
MICB (330)
ISG20 (194)
LY6E (187)
RTP4 (8)
RGL-1 (596)
PSRC1 (215)
SLFN5 (81)
KIAA0082 (256)
C22orf28 (124)
PML (172)
IFIT1 (239)
OAS2 (158)
IRF2 (296.1)
NUP50 (110)
BLVRA (267)
PMAIP1 (16)
UBE2L6 (189)
RASSF4 (295)
IFIT2 (364)
CLEC2B (348)
ZNF385B (305)
EPSTI1 (75)
SPSB1 (205)
ARG2 (89)
C4orf33 (54)
CASP7 (210)
SERPING1 (121)
MAX (359)
G6PC (91)
NT5C3 (327)
SAT1 (44)
HK2 (258)
AMPH (154)
SLC1A1 (132)
APOL3 (218)
EIF2AK2 (10)
ZNF295 (324)
N4BP1 (356)
TREX1 (276)
HERC5 (513)
IFITM1 (33)
SLFN12 (144)
TAP1 (255)
FKBP5 (233)
BIRC3 (151)
SQLE (141)
GBP2 (150)
RAB27A (198)
SERPINE1 (226)
PUS1 (103)
IFI44L (99)
SAMD4A (304)
NCF1 (355)
BLZF1 (316)
NMI (269)
CCL19 (26)
VEGFC (228)
DNAPTP6 (321)
CCL8 (28)
PLSCR1 (7)
FCGR1A (94)
CD74 (200)
LGMN (283)
PLEKHA4 (168)
TYMP (117)
RARRES3 (263)
IFI6 (3)
CMAH (19)
SPTLC2 (138)
TLR3 (173)
CFB (166)
RNF19B (243)
PDGFRL (223)
PRKD2 (342)
TRIM14 (107)
IL28RA (386)
STAT2 (341)
CCND3 (350)
HLA-C (365)
GK (131)
TNFSF10 (69)
ABTB2 (170)
CXCL10 (25)
GPX2 (48)
FAM70A (86)
CD69 (53)
TRIM25 (289)
MAP3K5 (183)
NOD2 (310)
MYD88 (268)
TLR7 (179)
MDA5 (9)
IRF7 (113)
cGAS (379)
Mx2 (252)
ZBP1 (104)
RIPK2 (242.1)
RIPK2 (242)
IFITM3 (5)
IRF1 (270)
TRIM38 (235)
TRIM5 (240)
FAM46C (96)
FAM46A (333)
CDKN1A (191)
HPSE (136)
UNC84B (322)
PBEF1 (119)
CES1 (140)
NOS2A (181)
C5orf39 (294)
TRIM56 (165)
MKX (88)
CCR1 (90)
CX3CL1 (315)
C9orf91 (326)
SLC25A28 (274)
B4GALT5 (332)
CPT1A (282)
GJA4 (271)
CNP (229)
THBD (142)
TBX3 (339)
APOL6 (83)
SLC15A3 (287)
EXT1 (163)
UNC93B1 (307)
OAS3 (373)
GALNT2 (285)
FFAR2 (217)
MOV10 (177)
*
Screen Average
Inhibition
Enhancement
0
100
500
ND

Figure S2

Figure S2. Heat map representing effects of human ISGs on retroviral infection (Related to Figure 1 and Figure 2). The effect of ISGs in the 25 incoming and outgoing screens represented in a heat map. All screens were normalised to the screen average (100 arbitrary units) with inhibition indicated in red and enhancement in green. Absent data, due to inefficient transduction, is indicated in grey (ND). Where allelic variants, spliced variants and repeated genes occur in the library, all data is presented and represent separate values from distinct transduction/transfection events. Asterisks denote clusters of ISGs whose protective effect is most evident in THP-1 cells. Heatmaps were produced using Gitools 2.2 and genes were hierarchically clustered using Manhattan maximum distance.

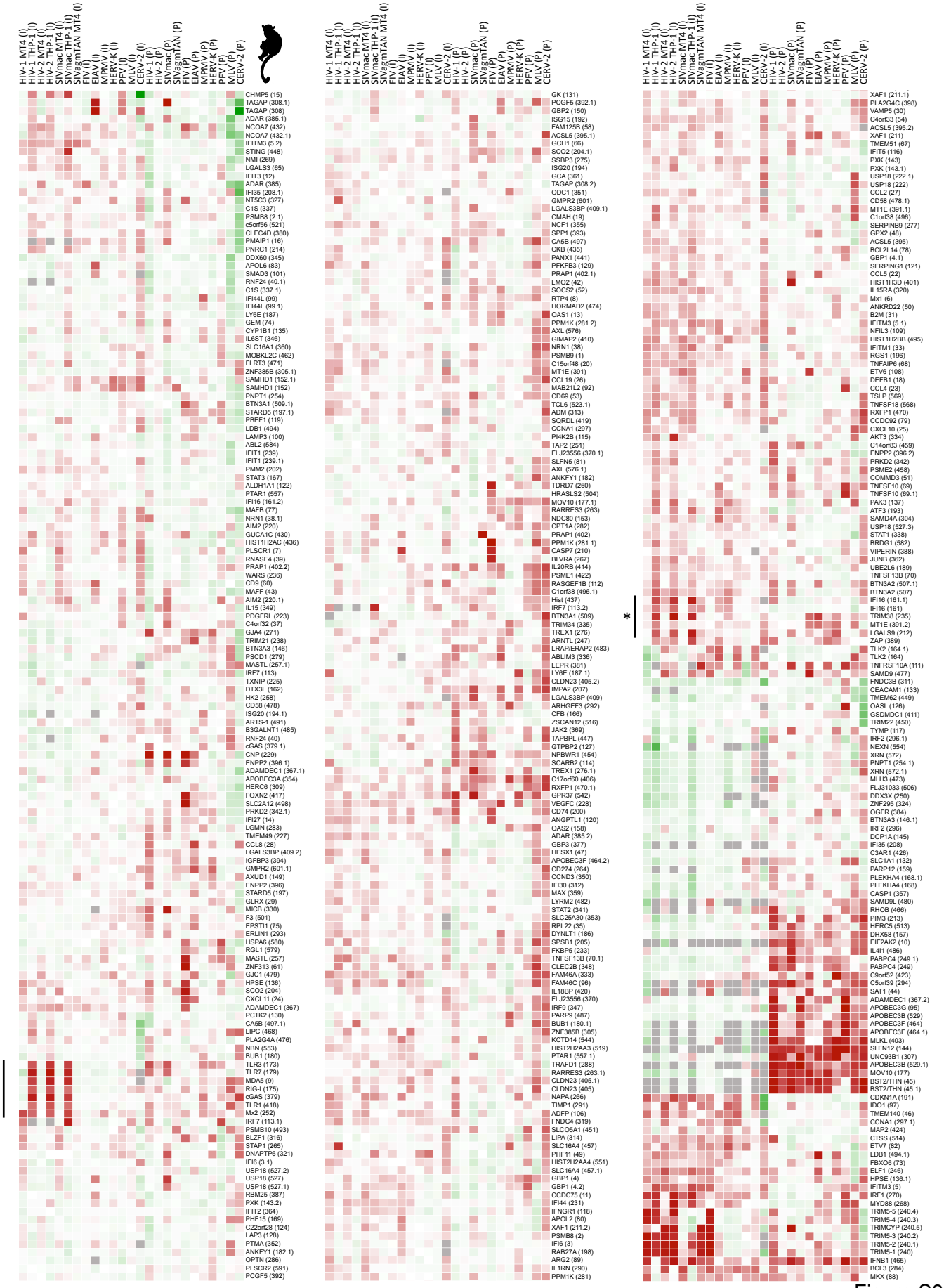
Incoming
Production
HIV-1 MT4 (I)
HIV-1 THP-1 (I)
HIV-2 MT4 (I)
HIV-2 THP-1 (I)
SIVmac MT4 (I)
SIVmac THP-1 (I)
SIVagmTAN MT4 (I)
FIV (I)
EIAV (I)
MPMV (I)
HERV-K (I)
PFV (I)
MLV (I)
CERV-2 (I)
HIV-1 (P)
HIV-2 (P)
SIVmac (P)
SIVagmTAN (P)
FIV (P)
EIAV (P)
MPMV (P)
HERV-K (P)
PFV (P)
MLV (P)
CERV-2 (P)
CHMP5 (15)
TAGAP (308.1)
TAGAP (308)
ADAR (385.1)
NCOA7 (432)
NCOA7 (432.1)
IFITM3 (5.2)
STING (448)
NMI (269)
LGALS3 (65)
IFIT3 (12)
ADAR (385)
IFI35 (208.1)
NT5C3 (327)
C1S (337)
PSMB8 (2.1)
c5orf56 (521)
CLEC4D (380)
PMAIP1 (16)
PNRC1 (214)
DDX60 (345)
APOL6 (83)
SMAD3 (101)
RNF24 (40.1)
C1S (337.1)
IFI44L (99)
IFI44L (99.1)
LY6E (187)
GEM (74)
CYP1B1 (135)
IL6ST (346)
SLC16A1 (360)
MOBKL2C (462)
FLRT3 (471)
ZNF385B (305.1)
SAMHD1 (152.1)
SAMHD1 (152)
PNPT1 (254)
BTN3A1 (509.1)
STARD5 (197.1)
PBEF1 (119)
LDB1 (494)
LAMP3 (100)
ABL2 (584)
IFIT1 (239)
IFIT1 (239.1)
PMM2 (202)
STAT3 (167)
ALDH1A1 (122)
PTAR1 (557)
IFI16 (161.2)
MAFB (77)
NRN1 (38.1)
AIM2 (220)
GUCA1C (430)
HIST1H2AC (436)
PLSCR1 (7)
RNASE4 (39)
PRAP1 (402.2)
WARS (236)
CD9 (60)
MAFF (43)
AIM2 (220.1)
IL15 (349)
PDGFRL (223)
C4orf32 (37)
GJA4 (271)
TRIM21 (238)
BTN3A3 (146)
PSCD1 (279)
MASTL (257.1)
IRF7 (113)
TXNIP (225)
DTX3L (162)
HK2 (258)
CD58 (478)
ISG20 (194.1)
ARTS-1 (491)
B3GALNT1 (485)
RNF24 (40)
cGAS (379.1)
CNP (229)
ENPP2 (396.1)
ADAMDEC1 (367.1)
APOBEC3A (354)
HERC6 (309)
FOXN2 (417)
SLC2A12 (498)
PRKD2 (342.1)
IFI27 (14)
LGMN (283)
TMEM49 (227)
CCL8 (28)
LGALS3BP (409.2)
IGFBP3 (394)
GMPR2 (601.1)
AXUD1 (149)
ENPP2 (396)
STARD5 (197)
GLRX (29)
MICB (330)
F3 (501)
EPSTI1 (75)
ERLIN1 (293)
HSPA6 (580)
RGL1 (579)
MASTL (257)
ZNF313 (61)
GJC1 (479)
HPSE (136)
SCO2 (204)
CXCL11 (24)
ADAMDEC1 (367)
PCTK2 (130)
CA5B (497.1)
LIPC (468)
PLA2G4A (476)
NBN (553)
BUB1 (180)
TLR3 (173)
TLR7 (179)
MDA5 (9)
RIG-I (175)
cGAS (379)
TLR1 (418)
Mx2 (252)
IRF7 (113.1)
PSMB10 (493)
BLZF1 (316)
STAP1 (265)
DNAPTP6 (321)
IFI6 (3.1)
USP18 (527.2)
USP18 (527)
USP18 (527.1)
RBM25 (387)
PXK (143.2)
IFIT2 (364)
PHF15 (169)
C22orf28 (124)
LAP3 (128)
PTMA (352)
ANKFY1 (182.1)
OPTN (286)
PLSCR2 (591)
PCGF5 (392)
GK (131)
PCGF5 (392.1)
GBP2 (150)
ISG15 (192)
FAM125B (58)
ACSL5 (395.1)
GCH1 (66)
SCO2 (204.1)
SSBP3 (275)
ISG20 (194)
GCA (361)
TAGAP (308.2)
ODC1 (351)
GMPR2 (601)
LGALS3BP (409.1)
CMAH (19)
NCF1 (355)
SPP1 (393)
CA5B (497)
OKB (435)
PANX1 (441)
PFKFB3 (129)
PRAP1 (402.1)
LMO2 (42)
SOCS2 (52)
RTP4 (8)
HORMAD2 (474)
OAS1 (13)
PPM1K (281.2)
AXL (576)
GIMAP2 (410)
NRN1 (38)
PSMB9 (1)
C15orf48 (20)
MT1E (391)
CCL19 (26)
MAB21L2 (92)
CD69 (53)
TCL6 (523.1)
ADM (313)
SQRDL (419)
CCNA1 (297)
PI4KB (115)
TAP2 (251)
FLJ23556 (370.1)
SLFN5 (81)
AXL (576.1)
ANKFY1 (182)
TDRD7 (260)
HRASLS2 (504)
MOV10 (177.1)
RARRES3 (263)
NDC80 (153)
CPT1A (282)
PRAP1 (402)
PPM1K (281.1)
CASP7 (210)
BLVRA (267)
IL20RB (414)
PSME1 (422)
RASGEF1B (112)
C1orf38 (496.1)
Hist (437)
IRF7 (113.2)
BTN3A1 (509)
TRIM34 (335)
TREX1 (276)
ARNTL (247)
LRAP/ERAP2 (483)
ABLIM3 (336)
LEPR (381)
LY86 (187.1)
CLDN23 (405.2)
IMPA2 (207)
LGALS3BP (409)
ARHGEF3 (292)
CFB (166)
ZSCAN18 (516)
JAK2 (369)
TAPBPL (447)
GTPBP2 (127)
NPBWR1 (454)
SCARB2 (114)
TRF2E (276.1)
C17orf60 (406)
RXFP1 (470.1)
GPR37 (542)
VEGFC (228)
CD74 (200)
ANXA2 (120)
OAS2 (158)
ADAR (385.2)
GBP3 (377)
HESX1 (47)
APOBEC3F (464.2)
CD274 (264)
CCND3 (350)
IFI30 (312)
MAX (359)
LYRM2 (482)
STAT2 (341)
SLC25A30 (353)
RPL22 (35)
DYNLT1 (186)
SPSB1 (205)
FKBP5 (233)
TNFSF13 (70.1)
CLEC2B (348)
FAM46A (333)
FAM46C (96)
IL18BP (420)
FLJ23556 (370)
IRF27 (347)
PARP9 (487)
BUB1 (180.1)
ZNF385B (305)
KCTD14 (544)
HIST2H2AA3 (519)
TIMP1 (557.1)
TRAFD1 (288)
RARRES3 (263.1)
CLDN23 (405.1)
CLDN23 (405)
NAPA (266)
TIMP1 (291)
ADFP (106)
FNDC4 (319)
SLCO5A1 (451)
LIPA (314)
SLC16A4 (457)
PHF11 (49)
HIST2H2AA4 (551)
SLC16A4 (457.1)
GBP1 (4)
GBP1 (4.2)
CCL7/C75 (11)
IFI44 (231)
IFNGR1 (118)
APOL2 (80)
XAF1 (211.2)
PSMB8 (2)
IFI6 (3)
RAB27A (198)
ARG2 (89)
IL1RN (290)
PPM1K (281)
XAF1 (211.1)
PLA2G4C (398)
VAMP5 (30)
C4orf33 (54)
ACSL5 (395.2)
XAF1 (211)
TMEM51 (67)
IFIT5 (116)
PXK (143)
PXK (143.1)
USP18 (222.1)
USP18 (222)
CCL2 (27)
CD58 (478.1)
MT1E (391.1)
C1orf38 (496)
SERPINB9 (277)
GPX2 (48)
ACSL5 (395)
BCL2L14 (78)
GBP1 (4.1)
SERPING1 (121)
CCL5 (22)
HIST1H3D (401)
IL15RA (320)
Mx1 (6)
ANKRD22 (50)
B2M (31)
IFITM3 (5.1)
NFIL3 (109)
HIST1H2BB (495)
IFITM1 (33)
RGS1 (196)
TNFAIP6 (68)
ETV6 (108)
DEFB1 (18)
CCL4 (23)
TSLP (599)
TNFSF18 (568)
RXFP1 (470)
CCDC92 (79)
CXCL10 (25)
AKT3 (334)
C14orf83 (459)
ENPP2 (396.2)
PRKD2 (342)
PSME2 (458)
COMMD3 (51)
TNFSF10 (69)
TNFSF10 (69.1)
PAK3 (137)
ATF3 (193)
SAMD4A (304)
USP18 (527.3)
STAT1 (338)
BRDG1 (582)
VIPERIN (388)
JUNB (362)
UBE2L6 (189)
TNFSF13B (70)
BTN3A2 (507.1)
BTN3A2 (507)
IFI16 (161.1)
IFI16 (161)
TRIM38 (235)
MT1E (391.2)
LGALS9 (212)
ZAP (389)
TLK2 (164.1)
TLK2 (164)
TNFRSF10A (111)
SAMD9 (477)
FNDC3B (311)
CEACAM1 (133)
TMEM62 (449)
OASL (126)
GSDMDC1 (411)
TRIM22 (450)
TYMP (117)
IRF2 (296.1)
NEXN (554)
XRN (572)
PNPT1 (254.1)
XRN (572.1)
MLH3 (473)
FLJ31033 (506)
DDX3X (250)
ZNF295 (324)
OGFR (384)
BTN3A3 (146.1)
IRF2 (296)
DCP1A (145)
IFI35 (208)
C3AR1 (426)
SLC1A1 (132)
PARP12 (159)
PLEKHA4 (168.1)
PLEKHA4 (168)
CASP1 (357)
SAMD9L (480)
RHOB (466)
PIM3 (213)
HERC5 (513)
DHX58 (157)
EIF2AK2 (10)
IL4I1 (486)
TNFSF14 (249.1)
PABPC4 (249)
C9orf52 (423)
C5orf39 (294)
SAT1 (44)
ADAMDEC1 (367.2)
APOBEC3G (95)
APOBEC3B (529)
APOBEC3F (464)
APOBEC3F (464.1)
MLKL (403)
SLFN12 (144)
UNC93B1 (307)
APOBEC3B (529.1)
MOV10 (177)
BST2/THN (45)
BST2/THN (45.1)
CDKN1A (191)
IDO1 (97)
TMEM140 (46)
CCNA1 (297.1)
MAP2 (424)
CTSS (514)
ETV7 (82)
LDB1 (494.1)
FBXO6 (73)
ELF1 (246)
HPSE (136.1)
IFITM3 (5)
IRF1 (270)
MYD88 (268)
TRIM5-5 (240.4)
TRIM5-4 (240.3)
TRIMCYP (240.5)
TRIM5-3 (240.2)
TRIM5-2 (240.1)
TRIM5-1 (240)
IFNB1 (465)
BCL3 (284)
MKX (88)
*
*

Figure S3

Figure S3. Heat map representing effects of macaque ISGs on retroviral infection (Related to Figure 1 and Figure 2). The effect of ISGs in the 25 incoming and outgoing screens represented in a heat map. All screens were normalised to the screen average (100 arbitrary units) with inhibition indicated in red and enhancement in green. Absent data, due to inefficient transduction, is indicated in grey (ND). Where allelic variants, spliced variants and repeated genes occur in the library, all data is presented and represent separate values from distinct transduction/transfection events. Asterisks denote clusters of ISGs whose protective effect is most evident in THP-1 cells. Heatmaps were produced using Gitools 2.2 and genes were hierarchically clustered using Manhattan maximum distance.

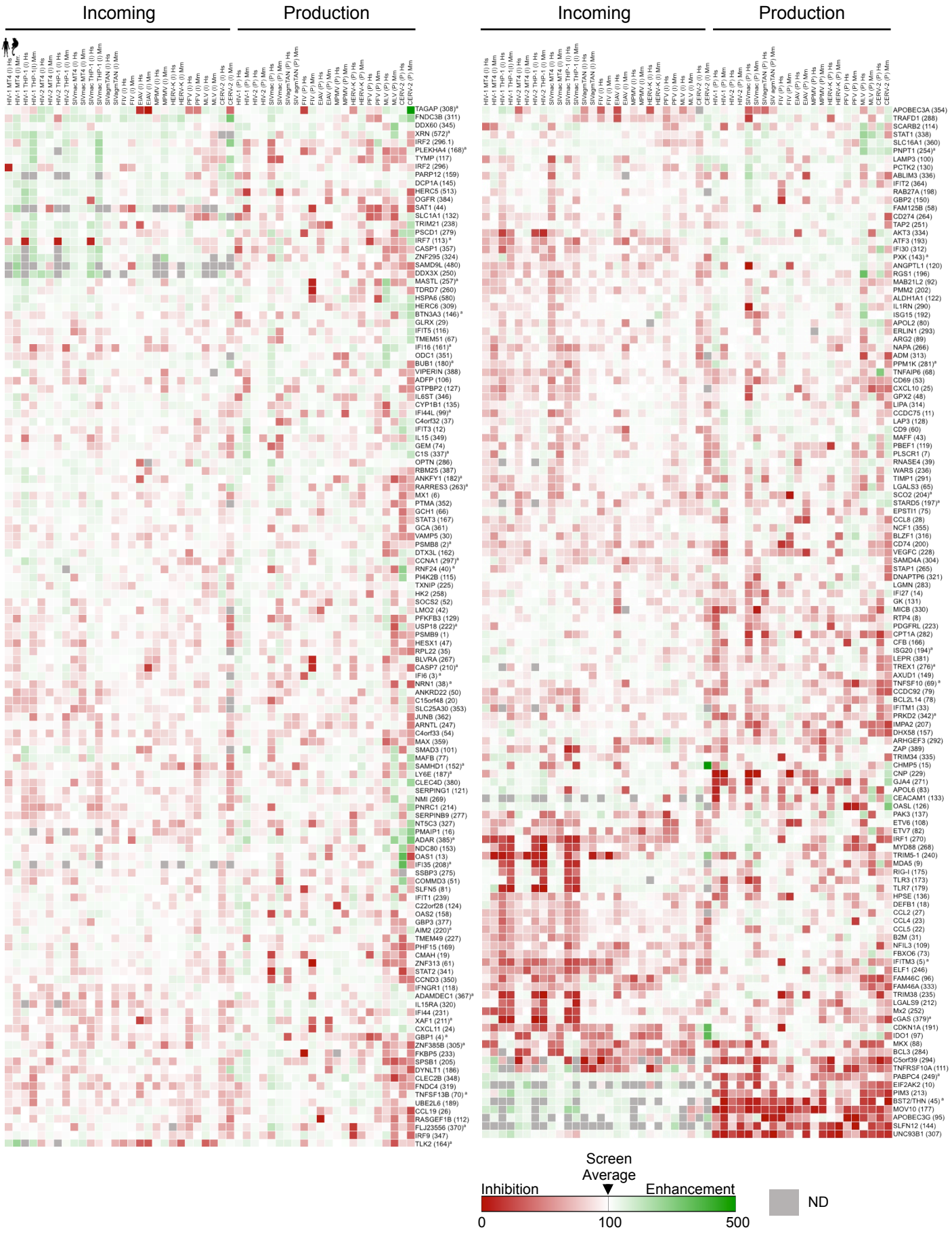
Incoming
Production
Incoming
Production
Screen Average
Inhibition
Enhancement
0
100
500
ND

Figure S4

Figure S4. Heat map comparing effects of human and macaque ISGs on retroviral infection (Related to Figure 1 and Figure 2). The effect of ISGs present in both human and macaque libraries in the 25 incoming and outgoing screens represented in a heat map (human left, macaque right for each screen). All screens were normalised to the screen average (100 arbitrary units) with inhibition indicated in red and enhancement in green. Absent data, due to inefficient transduction, is indicated in grey (ND). Where allelic variants, spliced variants and repeated genes occur in the library, all data is presented and represent separate values from distinct transduction/transfection events. Heatmaps were produced using Gitools 2.2 and genes were hierarchically clustered using Manhattan maximum distance.

[a] Multiple library copies (PSMB8, IFI16, GBP1, NRN1, RNF24, THN, TNFSF10, TNFSF13B, IRF7, HSPE, PXK, BTN3A3, SAMHD1, IFI16, PLEKHA4, MOV10, BUB1, IFI44L, ANKFY1, LY6E, ISG20, STARD5, SCO2, AIM2, IFI35, CASP7, XAF1, USP18, PABPC4, RARRES3, PNPT1, MASTL, TREX1, PPM1K, CCNA1, TAGAP, PRKD2, C1S, ADAMDEC1, FLJ23556, cGAS, ADAR, XRN)

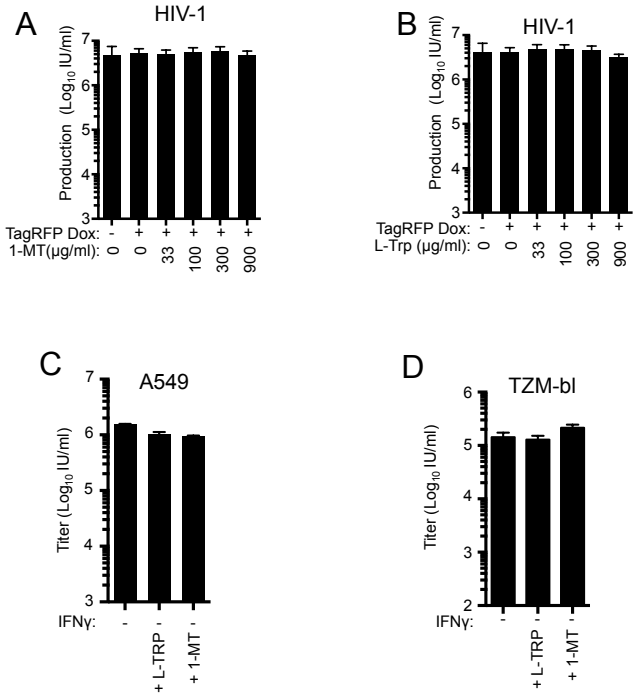
A
HIV-1
Production (Log10 IU/ml)
TagRFP Dox: - + + + + +
1-MT(μg/ml): 0 0 33 100 300 900
B
HIV-1
Production (Log10 IU/ml)
TagRFP Dox: - + + + + +
L-Trp (μg/ml): 0 0 33 100 300 900
C
A549
Titer (Log10 IU/ml)
IFNγ: - - + L-TRP - + 1-MT
D
TZM-bl
Titer (Log10 IU/ml)
IFNγ: - - + L-TRP - + 1-MT

Figure S5

Figure S5. 1MT and L-Trp do not affect HIV-1 replication without IDO1 induction or IFNγ treatment (Related to Figure 4 and Figure 5).

(A, B) Effects of 1-MT (A) or L-Trp (B) on the yield of infectious HIV-1 particles during a single cycle of HIV-1 replication in control MT4 cells (containing doxycycline inducible TagRFP)

(C) The yield of infectious progeny virions from a single cycle of HIV-1 replication in A549 cells without IFN-γ treatment in the presence of 50 μg/ml L-Trp or 100 μg/ml 1-MT

(D) As in C with TZM-bl cells, using 33 μg/ml L-Trp (TZM-bl cells) or 100 μg/ml 1-MT. Titers are mean+SD

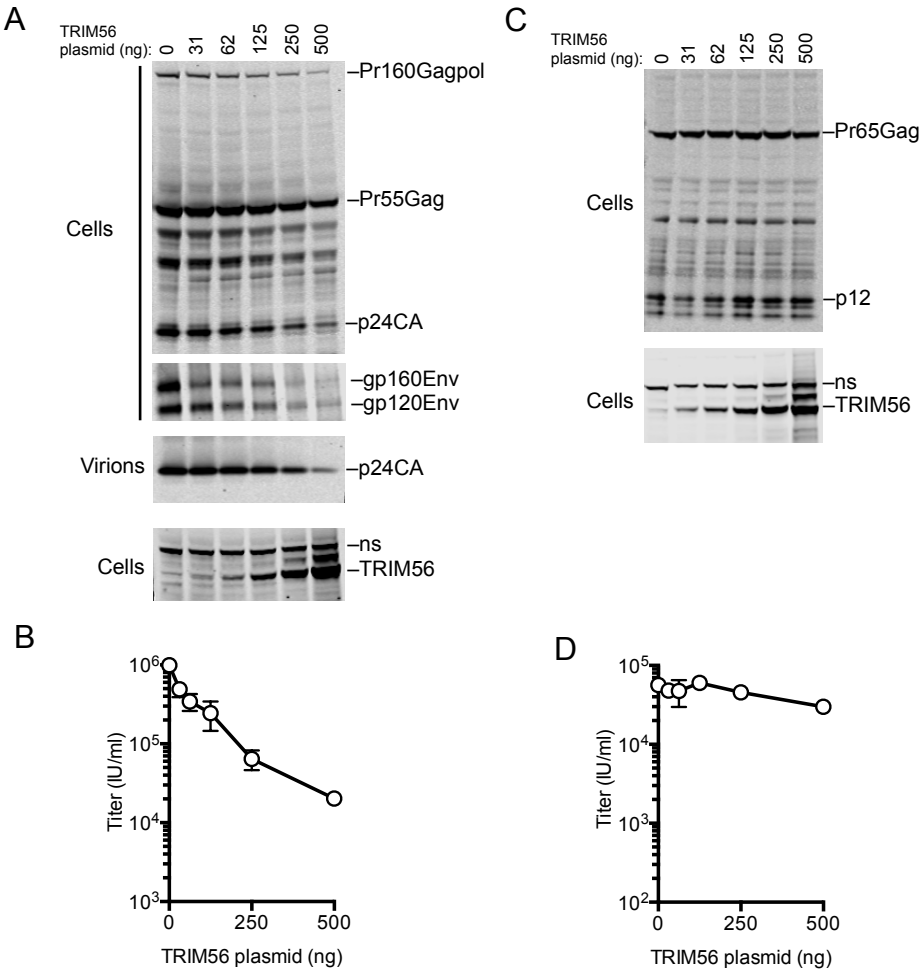
A
TRIM56
plasmid (ng):
0
31
62
125
250
500
Pr160Gagpol
Pr55Gag
p24CA
Cells
gp160Env
gp120Env
Virions
p24CA
Cells
ns
TRIM56
C
TRIM56
plasmid (ng):
0
31
62
125
250
500
Pr65Gag
Cells
p12
Cells
ns
TRIM56
E
Virion p24 (a.u.)
6
5
4
3
0.5
0.25
B
Titer (IU/ml)
10^6
10^5
10^4
10^3
0
250
500
TRIM56 plasmid (ng)
D
Titer (IU/ml)
10^5
10^4
10^3
10^2
0
250
500
TRIM56 plasmid (ng)

Figure S6

Figure S6. Effects of TRIM56 on HIV-1 replication (Related to Figure 6).
(A) Western blot analysis of HIV-1 Gag, Env and TRIM56 expression and particle release following transient cotransfection of 293T cells with HIV-1 proviral plasmids and increasing amounts of a TRIM56 expression plasmid.
(B) Western blot analysis of MLV Gag and TRIM56 expression and particle release following transient cotransfection of 293T cells with MLV GagPol and vector plasmids, along with VSV-G and increasing amounts of a TRIM56 expression plasmid.
(C) The yield of infectious HIV-1 virions from cells transfected in panel (A).
(D) The yield of infectious MLV virions from cells transfected in panel (B).
(E) Quantitation of virion associated p24 CA generated in a single cycle of infection of GHOSTX4 and GHOSTX4-TRIM56 cells. Titers are mean+SD

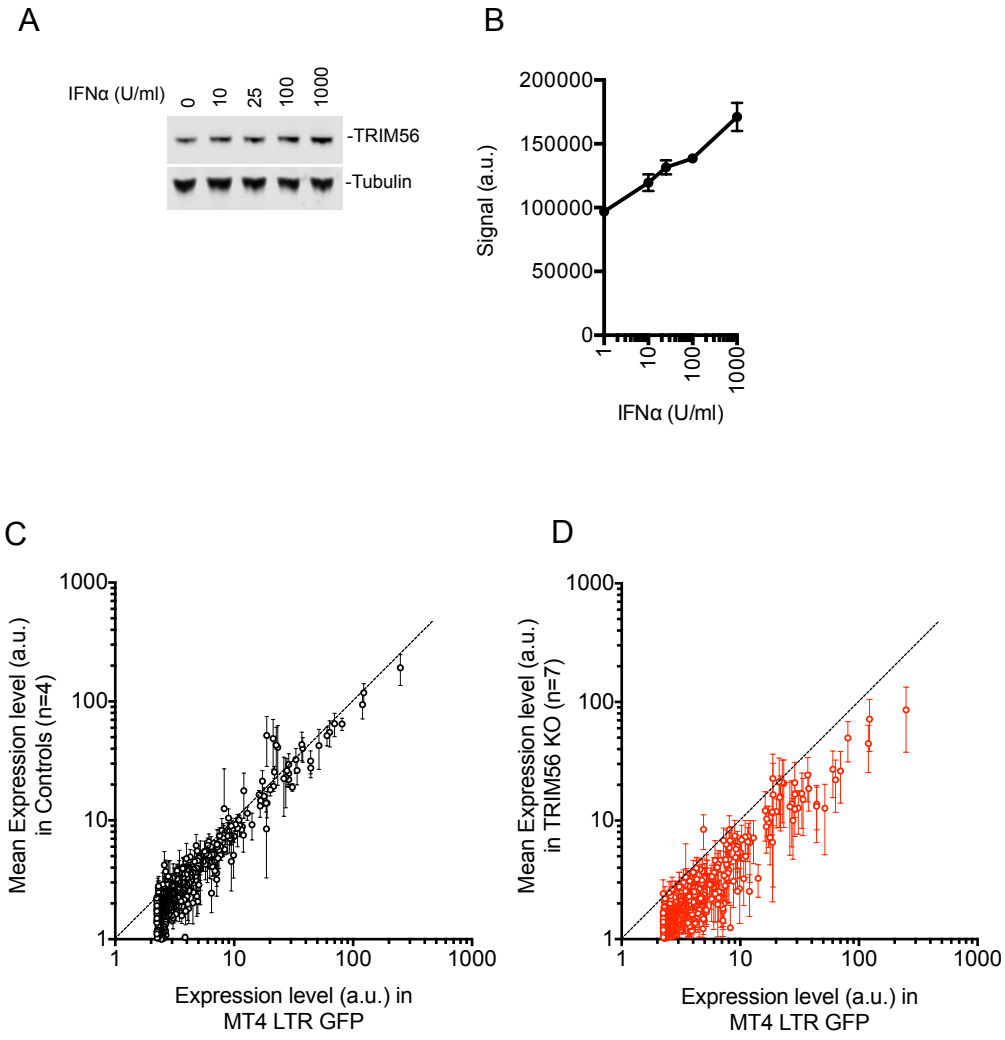
A
IFNα (U/ml)
0
10
25
100
1000
-TRIM56
-Tubulin
B
Signal (a.u.)
200000
150000
100000
50000
0
1
10
100
1000
IFNα (U/ml)
C
Mean Expression level (a.u.) in Controls (n=4)
Expression level (a.u.) in MT4 LTR GFP
D
Mean Expression level (a.u.) in TRIM56 KO (n=7)
Expression level (a.u.) in MT4 LTR GFP

Figure S7

Figure S7. Induction of TRIM56 and ISG expression by IFNα (Related to Figure 7).
(A, B) Western blot analysis of TRIM56 protein levels in MT4-LTR-GFP cells treated with increasing doses of IFNα. A typical blot (A) and quantitiation (B) is shown (B, mean ± SD).
(C, D) Microarray analysis of the expression levels (in arbitrary units, a.u.) of 500 genes induced by 25U/ml IFNα in unmodifed MT4-LTR-GFP cells (X-axis) versus corresponding mean values (Y-axis) for clones of control (C, mean ± SD n=4) or TRIM56-knockout (D, mean ± SD, n=7) MT4-LTR-GFP cells. The diagonal dashed lines indicate positions on which data points would fall if values were equivalent in the two plotted datasets.

Table S1. Viral plasmids and target cells for ISG screens (Related to Figures 1 and 2)

			Target cells	
Virus	**Plasmid(s)**	**Reference(s)**	**Incoming screens**	**Outgoing[a] Screens**
HIV-1	pNHG (JQ585717)/VSV-G	(Wilson et al., 2012)	MT4, THP-1	n/a
	pNL4.3 (M19921)	(Adachi et al., 1986)	n/a	MT4-TMZ[b]
HIV-2	Δ*nef*Δ*env* EGFP/VSV-G	(Hatziioannou et al., 2003)	MT4, THP-1	MT4
SIVmac	Δ*nef*Δ*env* EGFP/VSV-G	(Hatziioannou et al., 2003)	MT4, THP-1	MT4
SIVagmTAN	Δ*nef*Δ*env* EGFP/VSV-G	(Hatziioannou et al., 2003)	MT4	MT4
FIV	Gag-Pol/packageable genome /VSV-G	(Kemler et al., 2002)	MT4	MT4
EIAV	Gag-Pol/packageable genome /VSV-G	(Mitrophanous et al., 1999)	CRFK	MT4
MPMV	pSARM-EGFP/VSV-G	(Newman et al., 2006)	MT4	MT4
HERV-K	Gag-Pol/K-rec/packageable genome /VSV-G	(Lee and Bieniasz, 2007)	MT4	293T
MLV	Gag-Pol/packageable genome /VSV-G	(Soneoka et al., 1995) (Neil et al., 2001)	MT4	MT4
CERV-2/MLV	CERV2/MLV chimeric Gag-Pol/packageable genome /CERV2-Env	(Perez-Caballero et al., 2008; Soll et al., 2010)	293T	293T
PFV[a]	Δ*bet*Δ*bel3* 2A-EGFP	(Bock et al., 1998; Schmidt and Rethwilm, 1995)	HT1080	HT1080

[a] HEK 293T cells were used as producer cells for all outgoing screens with the exception of PFV, in which HT1080s were used.
[b] MT4 TMZ cells are a single cell clone derived from MT4 cells that encode an HIV-1 LTR-GFP reporter construct [T.M. Zang and P.D. Bieniasz, unpublished data and (Busnadiego et al., 2014)]

Table S2. ISG-encoding vectors with low titer (Related to Figures 1 and 3)

SPECIES	ISG	Antiretroviral? [b]	TRANSDUCTION (MT4)[a]	TRANSDUCTION (THP-1)[a]
Human	MDA5	IFN hit	44.10	13.32
Human	EIF2AK2	YES	27.15	2.19
Human	IFITM1	No	71.05	6.85
Human	RNASE4	No	113.75	8.97
Human	RNF24	No	90.62	19.45
Human	SAT1	No	7.71	1.06
Human	BST2/THN	YES	64.18	2.52
Human	FLJ11286	No	92.52	15.81
Human	APOBEC3G	YES	0.36	0.66
Human	TNFRSF10A	IFN Hit	29.82	2.98
Human	CEACAM1	YES	1.06	0.26
Human	FUT4	No	104.85	15.74
Human	SLFN12	YES	0.97	0.55
Human	DCP1A	No	91.00	14.00
Human	PARP12	No	66.09	4.24
Human	TLK2	YES	56.61	4.60
Human	TRIM56	YES	14.48	12.29
Human	PLEKHA4	No	105.49	11.93
Human	MAP3K14	IFN hit	98.12	3.82
Human	MOV10	YES	5.84	1.83
Human	NOS2A	YES	4.56	1.02
Human	STARD5	No	112.73	8.15
Human	FFAR2	YES	64.95	16.88
Human	DDX3X	No	1.26	3.29
Human	IRF1	IFN hit	96.08	12.50
Human	TREX1	YES	89.86	9.10
Human	BCL3	YES	107.01	9.35
Human	C5orf39	YES	10.88	13.03
Human	UNC93B1	YES	85.79	11.98
Human	IL15RA	No	100.40	8.44
Human	ZNF295	No	19.38	3.36
Human	CASP1	No	27.91	7.35
Human	ADAMDEC1	YES	103.71	18.36
Human	OAS3	YES	20.47	3.39
Human	ABCA9	No	22.80	0.44
Human	SAMD9L	No	0.60	2.14
Human	PARP10	No	36.86	5.24
Human	HERC5	No	99.01	13.15
Human	TGFB1	IFN hit	103.58	19.06
Human	TNK2	YES	61.26	7.06
Macaque	EIF2AK2	YES	0.08	0.39
Macaque	PMAIP1	No	61.49	2.23
Macaque	RNF24	No	84.49	10.76
Macaque	RNF24[c]	No	74.24	4.16
Macaque	SAT1	No	10.71	0.95
Macaque	BST2/THN	YES	1.07	0.85
Macaque	BST2/THN[c]	YES	1.35	2.27
Macaque	APOBEC3G	YES	63.62	17.99
Macaque	TNFRSF10A	IFN Hit	20.51	1.97
Macaque	IRF7	IFN Hit	101.11	12.11
Macaque	IRF7[c]	IFN Hit	93.61	3.73
Macaque	IRF7[c]	IFN Hit	85.11	1.20
Macaque	CEACAM1	YES	60.74	3.96
Macaque	SLFN12 (isoform 2)	YES	0.85	1.31
Macaque	PARP12	No	85.36	5.61
Macaque	TLK2	YES	22.75	12.77
Macaque	MOV10	YES	18.57	16.15
Macaque	ISG20	No	64.62	9.89
Macaque	IFI35	No	6.47	0.66
Macaque	DDX3X	No	14.75	20.33
Macaque	C5orf39	YES	3.25	5.73
Macaque	UNC93B1	YES	100.11	12.26
Macaque	ZNF295	No	30.93	11.61
Macaque	C6orf150	YES	84.61	10.75
Macaque	MLKL	YES	8.92	0.23
Macaque	APOBEC3F	YES	29.42	0.84
Macaque	APOBEC3F[c]	YES	39.49	0.70
Macaque	RHOB	No	3.18	3.91
Macaque	SAMD9L	YES	3.32	63.70
Macaque	BTN3A1	YES	2.48	0.60
Macaque	APOBEC3B	No	5.18	14.73

[a] Normalized transduction (% of screen average)
[b] Stimulated IFNβ/ISRE driven reporter activity (IFN hit), Appears (yes) or does not appear (No) in Table S1 (ISGs with antiretroviral activity)
[c] Multiple library copies (RNF24, THN, IRF7, APOBEC3F)

Table S3. Human ISGs subtracted due to ISRE or IFNβ promoter stimulation (Related to Figure 3)

ISG	IFNβ 293T[a]	IFNβ THP1[a]	ISRE 293T[a]
EPSTI1	9.87	1.59	0.50
IL1R	0.73	24.71	0.65
IRF1	11.41	1.33	74.83
IRF7	1.40	0.91	65.14
MAFF	0.68	1.46	6.83
MAP3K14	365.11	39.42	49.44
MAP3K5	1.72	34.32	0.20
MDA5	10.88	1.16	51.38
MYD88	192.01	44.87	1.75
NOD2	22.38	6.88	0.55
P2RY6	6.04	1.88	3.02
RIG-I	3.80	1.12	6.12
RIPK2	85.93	36.50	0.68
RIPK2[b]	112.12	140.93	1.15
TBX3	1.59	0.71	7.02
TGFB1	21.40	1.25	0.69
TLR7	0.64	15.66	1.74
TNFRSF10A	243.76	0.63	3.22
TRIM25	43.36	85.06	0.06
TRIM38	12.16	12.37	0.85

[a] Fold-activation of reporter gene expression
[b] Two library copies (RIPK2)

Table S4. Macaque ISGs subtracted due to ISRE or IFNβ promoter stimulation (Related to Figure 3)

ISG	IFNβ 293T[a]	IFNβ THP1[a]	ISRE 293T[a]
AIM2	0.92	22.92	1.06
AIM2[b]	1.31	15.62	0.98
IFI16	0.81	8.83	0.38
IFNB1	0.75	1.31	62.74
IRF1	11.56	0.85	63.34
IRF7	2.24	9.49	29.32
IRF7[b]	2.85	20.08	14.72
MYD88	11.09	17.13	1.24
PRKD2	0.99	7.39	0.46
RIG-I	10.58	0.40	4.25
TNFRSF10A	28.80	0.63	5.64
TRIM38	1.27	14.34	0.98
TRIM5-5	1.17	7.88	1.06

[a] Fold-activation of reporter gene expression
[b] Two library copies (AIM2 and IRF7)

Table S5. ISGs with anti-retroviral activity (Related to Figure 1, Figure 2, and Figure S1).

ISG[a]	Incoming Screens (Hs)[b]	Incoming Screens (Mm)[b]	Production Screens (Hs)[c]	Production Screens (Mm)[c]	Anti-SCRPSY[d]	Reported anti-retroviral activity[e]	Reference(s)
IDO1	HIV-2(MT4)	HIV-2(MT4)				Here	
TRIM56			HIV-1, HERV-K		Yes	Here	
ADAMDEC1				HIV-1, SIVagmTAN, PFV	Yes	No	
AKT3	HIV-1(THP-1), HIV-2(THP-1)	HIV-2(THP-1)				No	
ANGPTL1			SIVmac			No	
APOBEC3A	EIAV, HERV-K					Yes	(Berger et al., 2011)
APOBEC3B				HIV-1, HIV-2, SIVmac, PFV SIVagmTAN, MLV, CERV-2		Yes	(Yu et al., 2004)
APOBEC3F				HIV-1, SIVagmTAN, PFV	Yes	Yes	(Wiegand et al., 2004)
APOBEC3G			SIVagmTAN, FIV, PFV	SIVagmTAN, PFV, HIV-1	Yes	Yes	(Sheehy et al., 2002)
APOL1			FIV			Yes	(McLaren et al., 2015; Taylor et al., 2014)
APOL6	SIV(THP-1)	EIAV	HIV-1, MPMV			Yes	(McLaren et al., 2015)
B4GALT5			EIAV			No	
BCL3	HIV-2(MT4), SIVmac(MT4), FIV	HIV-2(MT4), SIVmac(MT4), FIV			Yes	Yes	(Hishiki et al., 2007)
BIRC3			FIV			No	
BLVRA				FIV		No	
BST2/THN[f]			SIVmac, MLV	SIVmac, MLV, HIV-1, FIV, EIAV, MPMV, CERV-2	Yes	Yes	(Neil et al., 2008)
BTN3A1				CERV-2	Yes	No	
C17orf60				MPMV		No	
C22orf28			MPMV			No	
C5orf39	HIV-2(MT4), SIVmac(THP-1), FIV		HERV-K, CERV-2	HIV-1, SIVmac	Yes	No	
C9orf52				HERV-K		No	
CASP7		EIAV	FIV			No	
CCR1			FIV, EIAV, HERV-K			No	
CD163			HERV-K			No	
CD74			FIV			Yes	(Schoggins et al., 2015)
CDKN1A		HIV-1(MT4), HIV-2(THP-1)	FIV			Yes	(Pauls et al., 2014)
CEACAM1			HIV-1		Yes	No	
CEBPD			SIVmac			No	
cGAS	SIVmac(THP-1), HIV-1(THP-1), HIV-2(THP-1)	SIVmac(THP-1), HIV-1(THP-1), HIV-2(THP-1)			Yes	PI	(Gao et al., 2013; Schoggins et al., 2014; Schoggins et al., 2015)
CHMP5	SIVmac(THP-1)					Yes	(Kuang et al., 2011; Pincetic et al., 2010)
CLEC2B				MLV		No	
CLEC4A	SIVmac(MT4)					No	
CNP			HIV-1, SIVmac	HIV-1, SIVmac, FIV		Yes	(Wilson et al., 2012)
CPT1A			SIVmac, EIAV, CERV-2			No	
CRY1			FIV			No	
CX3CL1			HIV-1, EIAV			No	
EHD4			HIV-1, EIAV			No	(Bregnard et al., 2013)
EIF2AK2				SIVmac	Yes	PI, Yes	(Deb et al., 2001; Yoon et al., 2015)
ELF1	SIVmac(THP-1)	HIV-2(MT4)				No	(Leiden et al., 1992)
ENPP2				FIV		No	
EPAS1	EIAV		HERV-K			No	
ETV7		MPMV				No	
EXT1			SIVmac, HERV-K, CERV-2			No	
FAM46A	MPMV					No	
FAM46C	HIV-1(THP-1), HIV-2(THP-1), HERV-K					No	(Telenti and Johnson, 2012)

FFAR2			HIV-1, HIV-2, SIVmac, SIVagmTAN, FIV, EIAV, MPMV, HERV-K, PFV, MLV, CERV-2		Yes	No	
FKBP5			FIV			No	
FLJ23556			HERV-K			No	
FOXN2				FIV		No	
GAK			MPMV			No	
GALNT2			HIV-1, SIVmac, FIV, CERV-2			No	
GBP2			FIV			No	
GJA4			HIV-1, SIVmac			No	
GPR37				HIV-1, SIVmac		No	
HIST1H3D				SIVmac		No	
HPSE				FIV		No	
MDA5		HIV-1(THP-1), HIV-2(THP-1), SIVmac(THP-1)				PI	(Andrejeva et al., 2004)
IFITM3	SIVmac(THP-1), HIV-1(THP-1)	SIVmac(THP-1), HIV-1(THP-1)	FIV			Yes	(Brass et al., 2009; Compton et al., 2014)
IL1RN			SIVmac			No	
IL4I1				SIVmac		No	
IRF2	HIV-1(MT4)					No	
IRF9			HERV-K			PI	(Randall and Goodbourn, 2008)
LAMP3	SIVmac(MT4)					No	
LDB1				EIAV		No	
LGALS9		HIV-2(THP1), SIVmac(THP-1)				PI	(Matsuura et al., 2009)
MACS			HIV-1			No	
MASTL				FIV		No	
MICB				SIVmac		No	
MKX	EIAV		HIV-1, SIVagmTAN			No	
MLKL				HIV-1, HERV-K, CERV-2, PFV	Yes	No	
MOV10			HIV-1, SIVmac, SIVagmTAN, FIV, MPMV, PFV, CERV-2	HIV-1, SIVmac, SIVagmTAN, FIV, MPMV	Yes	Yes	(Furtak et al., 2010; Wang et al., 2010)
Mx2	HIV-1(THP-1), HIV-2(THP-1), SIVmac(THP-1)	HIV-1(MT4), SIVmac(THP-1)				Yes	(Goujon et al., 2013; Kane et al., 2013; Liu et al., 2013)
NFIL3	SIVmac(THP-1)					No	
NOS2A	HIV-2(MT4)		HERV-K, CERV-2		Yes	No	
OAS3			CERV-2		Yes	No	
OASL			PFV	PFV		No	
PABPC4				HIV-1, SIVmac		No	
PAK3	PFV					No	(Nguyen et al., 2006)
PBEF1			HERV-K			No	
PIM3				HIV-1, CERV-2		No	
PPM1K				FIV		No	
PRAP1				SIVagmTAN		No	
RASGEF1B			EIAV			No	
RHOB				HIV-1	Yes	PI	(Xu et al., 2014)
RNF19B			HIV-1			No	
SAMD9		HIV-2(MT4)		FIV		No	
SCO2				FIV		No	
SLC15A3			HIV-1, SIVmac, MPMV, CERV-2			PI	(Nakamura et al., 2014)
SLC16A4		HIV-1(THP-1)				No	
SLC2A12				FIV		No	
SLFN12			HERV-K	HIV-1, HIV-2, SIVmac, HERV-K, EIAV, CERV-2, PFV	Yes	No	
SP100	SIVmac(THP-1)					No	
SQLE			FIV			No	
STAT2			SIVmac			PI	(Randall and Goodbourn, 2008)
TAGAP	EIAV	EIAV		SIVmac		No	
TDRD7				FIV		Yes	(Lu et al., 2011)
THBD			HIV-1			No	

TLK2		EIAV			Yes	No	
TLR1		HIV-2(THP-1)				PI	(Pasare and Medzhitov, 2005)
TLR3	SIVmac(THP-1)	HIV-1(THP-1), HIV-2(THP-1), SIVmac(THP-1)	SIVmac			PI	(Gibbert et al., 2014; Pasare and Medzhitov, 2005)
TLR7		HIV-1(THP-1), HIV-2(THP-1), SIVmac(THP-1)				PI	(Kane et al., 2011; Pasare and Medzhitov, 2005)
TMEM173		SIVmac(THP-1)				PI	(Burdette et al., 2011)
TNFSF10[f]				PFV		No	
TNK2			HIV-1		Yes	No	
TRAFD1	EIAV					No	
TREX1				SIVmac	Yes	No	(Yan et al., 2010)
TRIM34			FIV			Yes	(Zhang et al., 2006)
TRIM5[f]	HIV-1(THP-1), HIV-2(THP-1), SIVmac(THP-1)	HIV-1(MT4,THP-1), HIV-2(MT4,THP-1), SIVmac(THP-1),SIVagmTAN, FIV				Yes	(Stremlau et al., 2004)
TRIMCYP		HIV-2(MT4, THP-1), FIV, SIVagmTAN		SIVmac		Yes	(Sayah et al., 2004; Wilson et al., 2008)
ULK4			FIV			No	
UNC84B (SUN2)	HIV-1(THP-1), HIV-2(THP-1)					Yes	(Donahue et al., 2016; Lahaye et al., 2016)
UNC93B1			HIV-1, SIVmac, SIVagmTAN, HERV-K, MLV, CERV-2	HIV-1, HIV-2, SIVagmTAN, HERV-K, MLV, CERV-2, EIAV, MPMV	Yes	PI	(Kim et al., 2008)
USP18				SIVmac		No	
XAF1	EIAV					No	
ZC3HAV1	SIVmac(THP-1)	SIVmac(THP-1)				Yes	(Gao et al., 2002)
ZNF107			SIVagmTAN			No	
ZNF313				FIV		No	

[a] ISGs which stimulated the IFNβ or IRSE promoter (Figure 3 and Table S3 and S4) are subtracted from this list. Hyperlinks are to the UniProt entries of the human orthologue (not necessarily the isoform screened).

[b] Viruses inhibited by 3-fold or greater in incoming screens, cell type indicated in parenthesis for cases in which ISGs were tested in more than one screen.

[c] Viruses inhibited by 5-fold or greater in production screens.

[d] ISGs that affected titer/transduction of the SCRPSY vector (Figure S1 and Table S2) are indicated by “Yes”

[e] “PI” indicates genes reported to have pro-inflammatory activity such as activating anti-viral cytokine production/signaling

[f] Multiple library copies (TNFSF10, THN, TRIM5, PABPC4, TAGAP, APOBEC3F, APOBEC3B)

Extended Experimental Procedures

Cell lines

The feline CRFK cells, macaque FRhK4 and LLC-MK2 and adherent human HEK 293T, TE671 and TZM-bl cell lines were maintained in Dulbecco's Modified Eagle's Medium (DMEM) with 10% FBS and gentamicin. GHOSTX4 (a single cell clone of the original GHOSTX4R5 cell line obtained through the AIDS Reagent Program, Division of AIDS, NIAID, NIH from Dr. Vineet N. KewalRamani and Dr. Dan R. Littman) were maintained in DMEM supplemented with 2.5μg/ml puromycin, 50μg/ml hygromycin, and 500μg/ml G418. A549 cells were maintained in Ham's F12/DMEM, all supplemented with 9% fetal bovine serum (FBS) and gentamicin. Suspension rhesus 221 cells (RPMI supplemented with IL-2 and 17% FBS) and human MT4 and THP-1 cells were maintained in RPMI supplemented with 10% FBS and gentamicin. MT4-LTR-GFP indicator cells were generated by transduction with a lentivirus derived from pSIR LTR-GFP, a self-inactivating MLV reporter construct containing a cassette in which hrGFP expression is driven by the HIV-1 LTR. A single cell clone was generated by limiting dilution and maintained in 2.5μg/ml puromycin. ISG-expressing MT4 and GHOSTX4 cell lines were modified using lentiviral vectors. Limiting dilution was also used to generate a panel of GHOSTX4 cells, modified to express TRIM56. IFNβ1/ISRE reporter cell lines represent cell clones modified using MLV-derived retroviral vectors.

Retroviruses

Replication competent proviral clones encoding GFP (PFV) or VSV-G-pseudotyped envelope minus derivatives of HIV-1 (NHG Δ*env*/VSV-G), HIV-2 (HIV-2 Δ*env* EGFP/VSV-G), SIVmac (SIVmac Δ*nef* Δ*env* EGFP/VSV-G) and SIVagmTAN (Δ*nef* Δ*env* EGFP/VSV-G) or multi-plasmid VSV-G pseudotyped vector systems FIV, EIAV, HERV-K, and MLV were used as described previously (Busnadiego et al., 2014; Kane et al., 2013; Wilson et al., 2012). The 'CERV2' virus was generated using a chimeric construct containing a full length CERV2 Gag gene that is a consensus of endogenous CERV2 Gag sequences found in the chimpanzee genome (Perez-Caballero et al., 2008), linked to an MLV Pol sequence. CERV2 virions generated by co-transfection of 5μg of chimeric CERV2/MLV Gag-Pol, 5μg of MLV packageable genome, and 5μg of CERV2 envelope (Soll et al., 2010). In follow up analyses, intact proviral clones for HIV-1 (NL4-3) (M19921) and HIV-2 (ROD10) or GFP-encoding HIV-1 pNHG (JQ585717) with GFP in place of *nef* were also used. Intact proviral clones were pseudotyped with VSV-G as indicated.

Construction of an ISG library from rhesus macaques

An HIV-1 based vector pSCRPSY-DEST used to express the ISGs was based on a previously described HIV-1 based vector, pV1/hrGFP (Zennou and Bieniasz, 2006). pSCRPSY-DEST (GenBank accession KT368137) consists of a minimal packageable HIV-1 genome containing all essential *cis*-acting sequences with Gateway att^R and *Sfi*I restriction sites inserted in place of Nef, and a TagRFP-2A-$Puro^R$ cassette inserted in place of a deleted fragment containing *gag, pol, vif and vpr* genes. The *vpu* and *env* genes are also deleted or inactivated. Thus, cells transduced with pSCRPSY-DEST express HIV-1 Tat and Rev and any cDNA inserted into the DEST sequences from completely spliced 'early' HIV-1 transcripts, while TagRFP and PAC ($Puro^R$) are expressed from a late, unspliced HIV-1 transcript PAC2ATagRFP where PAC and TagRFP proteins are separated by a FMDV 2A stop-start peptide. In pilot experiments this vector format minimized the number of cells that expressed the transduction marker (TagRFP) but did not express a gene inserted into the DEST sites (typically EGFP).

Using the same criteria used to select human ISGs (Dittmann et al., 2015; Schoggins et al., 2011), primer pairs were designed to amplify ~600 different macaque genes by RT-PCR. In order to target genuine orthologous transcripts, multiple primer pairs were designed based on transcript variants of the most significant BLAST match of the rhesus macaque (*M. mulatta*) genome using human reference sequence ISGs as probes. Directional *Sfi*I restriction sites and 4 additional nucleotides were appended to the forward *Sfi*I oligos (5'-CTCT***GGCC****GAGAG****GGCC***ATG-3') and the final 3 nucleotides of the *Sfi*I site provided Kozak consensus sequences for the macaque ISGs. The reverse oligo also contained 4 additional nucleotides (5'-TCTC***GGCC****AGAGA****GGCC***TTA-3') and were immediately followed by the reverse complement of the ISG stop codon (ochre/UAA in this example). Each oligo also contained ~25 nucleotides complementary to the macaque ISG target. In total 864 primer pairs were designed and subsequently synthesized by Operon. IFNα-stimulated (1000 units/ml) FRhK4, LL-CMK2 and 221 cells were used as a source of macaque RNA (*M. mulatta*) for cDNA synthesis (superscript III). Pooled RNA from cells stimulated for 4, 16 and 24 hours was used. Each gene was PCR amplified using Pfu polymerase and reactions that did not yield the expected amplicon were repeated using Taq polymerase. PCR amplicons were conventionally cloned into a Gateway® (Invitrogen) compatible entry vector modified to contain directional *sfi*I sites. ISGs were subsequently sequence verified (Genewiz). ISG ORFs were selected for the library that either matched the amino acid sequence of NCBI macaque entries or yielded at least two clones with identical amino acid sequences. Selected ORFs were subcloned into pSCRPSY-DEST and pcDNA-

DEST40 (Invitrogen) destination vectors using LR-clonase (Invitrogen). The previously described arrayed human ISG library (Schoggins et al., 2011) was extended to include a small number of highly IFNα-stimulated human ISGs based upon the initial criteria used previously (Schoggins et al., 2011) and our own microarray data (Kane et al., 2013; Neil et al., 2008). This extended human library (Dittmann et al., 2015) was similarly transferred into pSCRPSY and pcDNA-DEST40 using LR-clonase. Prior to screening, the identity of human and macaque ISGs was confirmed using restriction digest (all clones) and scatter sequencing of ~10% of the libraries.

Screening ISGs for antiretroviral activity

For incoming screens, ISG-encoding lentiviral vectors (SCRPSY) were generated by cotransfection of 293T cells using polyethyleneimine with 25ng HIV-1 Gag-Pol and 5ng VSV-G expression vectors, along with 250ng of each SCRPSY-based ISG expression vector in a 96-well plate format ($0.35x10^5$ cells/well). Thereafter, culture supernatants were used to transduce the relevant susceptible target cells (THP-1 cells were spinoculated for 1hr at 1600 rpm). Transduced ISG-expressing cells were challenged 48 hours later with a single dose of the GFP-encoding retroviruses or retroviral vectors using a MOI ~0.5. Cells were fixed 48h post-infection and the percentage of TagRFP+ and GFP+ cells determined by flow cytometry. In order to determine ISGs that inhibit SCRPSY production (Figure S1 and Table S4, S5), the fraction of ISG/TagRFP-expressing cells was expressed as a percentage of the mean value across all wells for the respective library (*H. sapiens* or *M. mulatta*) in the HIV-1 incoming screens.

For production screens, 293T cells were transfected in a 96 well format, using polyethyleneimine with 75ng of ISG expression plasmids (pcDNA-DEST40) along with 5ng VSV-G expression vector, and 70ng of plasmids that generated GFP-transducing retroviruses (HIV-1, HIV-2, SIVmac, and SIVagmTAN), or 5ng of VSV-G with 35ng of Gag-Pol expression plasmid and 35ng of packageable genome (EIAV, FIV, and MLV), or 35 ng of chimeric CERV2/MLV Gag-Pol, 35ng of packeagable genome, and 35ng of CERV2-Env, or 7ng VSV-G with 50ng packageable genome, 38ng Gag-Pol, and 19ng K-Rec expression plasmids (HERV-K). At 48h after transfection, supernatants were harvested and used to challenge either MT4 cells (HIV-1, HIV-2, SIVmac, SIVagmTAN, EIAV, FIV, and MLV) or 293T cells (HERV-K and CERV2). For the PFV production screen, HT1080 cells were transfected with 75ng of ISG expression plasmids and 75ng PFV expression plasmid. At 48h post-transfection, cells were lysed by multiple freeze-thaws and lysates were used to challenge HT1080 cells. All cells were fixed 48h post-infection and the percentage of GFP+ cells determined by flow cytometry (see also Table S1).

For each ISG, the fraction of infected, ISG/TagRFP-expressing cells (incoming screens) or the yield of infectious virions (production screens) was expressed as a percentage of the mean value across all wells for the respective library (*H. sapiens* or *M. mulatta*) in a given screen, except the MPMV incoming screen, in which values are expressed as the mean value across each plate.

IFNβ1 and ISRE reporter cell lines and expression screens therein

We amplified the ISRE-Luc fragment containing 5 repeats of a canonical ISRE (ISRE - TAGTTTCACTTTCCC) from a pISRE-Luc plasmid (Agilent technologies, PathDetect ISRE cis Reporting System) using primers containing *Bgl*II sites and inserted this cassette upstream of the CMV IE promoter of pQCXIN (Clontech), in which NeoR has been replaced with the blasticidin resistant gene, termed pQCXIB. The plasmid used to make the reporter cell (ISRE-GFP) was constructed by insertion of 5 copies of the ISRE followed by the EGFP coding region into the *Bgl*II site, upstream of the CMV IE promoter of pQCXIB. The IFN beta promoter (-125 to +22) was amplified from human genomic DNA using primer pairs containing *Kpn*I at the 5'-end and *Hind*III at the 3'-end, respectively, and subcloned into pGL2-Luc (Promega). The IFN beta-Luc fragment was then amplified using primers containing *Bgl*II and subcloned into pQCXIB. To construct the reporter cells, we transduced 293T or THP-1, with a low multiplicity of infection (less than 0.1). After selection with blasticidin, limiting dilution and expansion, single clones were measured for luciferase activity upon IFNα treatment (for ISRE-GFP). Single responsive clones were chosen for the screening assays.

THP-1 and HEK 293T cells containing an IFN β-promoter-driven luciferase reporter were transduced with ISG libraries and luciferase activity measured 48hrs later with Luciferase Assay System (Promega E1501) using Modulus™ II (Turner BioSystems). To reflect total IFN β-promoter induction, these screens were not normalized and fold change is presented. HEK 293T cells containing the ISRE-driven GFP reporter were transduced with human and macaque ISG libraries, mock treated or treated with 100 units/ml IFNα, and GFP+ and RFP+ cells enumerated 12 hours later using flow cytometry. To reflect ISRE activation per transduced cell, these ISRE screens were normalized. ISGs stimulating ISRE/IFNB1 driven reporter expression by >5 fold (normalized to SCRPSY transduction levels) were excluded from further examination of the candidate 'directly acting inhibitors' of incoming retroviral infection and are listed in Table S2 and S3.

Stable or inducible expression of individual ISGs for follow–up studies

For constitutive expression of ISGs in follow up studies, a lentiviral vector CCIB was derived from CSGW by replacing sequences encoding GFP with a multi-cloning site followed by an IRES sequence and a blasticidin resistance cassette. The SFFV promoter was also replaced with a CMV promoter. A selection of genes that inhibited HIV-1 NL4-3 by 3-fold or more during an outgoing library screen were cloned into CCIB using *Sfi*I, *Pme*I-*Not*I, *Xmn*I/*Pme*I-*Not*I, *Pme*I or *Not*I restriction site combinations. These genes included the human FFAR, SLC15A3, TRIM56, APOL6, TBX3, EHD4, MOV10, GJA4, UNC93B1, TNK2, CX3CL1, MKX, MARCK, EXT1, CEACAM1 and OAS3, and the macaque MLKL, SLFN12, GPR37, PABPC4, C5ORF39, RHOB, SAT1, MOV10, GJA4 and UNC93B1. GHOSTX4 cell lines expressing each of the aforementioned ISGs that exhibited anti-HIV-1 activity in outgoing screens were generated by transduction with CCIB based viruses followed by selection with 5μg/ml blasticidin. A control cell line containing empty vector CCIB was similarly generated. Multiple single-cell clones of GHOSTX4 expressing TRIM56 cells were derived by limiting dilution, and the continued expression of CD4 and CXCR4 was verified using flow cytometry.

For doxycycline-inducible expression of ISGs, the modified tetracycline-inducible lentiviral expression vectors (pLKOΔ-Myc-TRIM5α-IP, pLKOΔ-Myc-TagRFP-IP, pLKOΔ-Myc-TRIM5α-IN, pLKOΔ-Myc-TagRFP-IN) have been previously described (Busnadiego et al., 2014). HsIDO1 was amplified from the human ISG library and cloned into the same lentiviral expression vectors to produce pLKOΔ-Myc-IDO1-IP and pLKOΔ-Myc-IDO1-IN using directional *Sfi*I sites. Doxycycline-inducible cell lines were produced via transduction of MT4 cells with modified LKO-derived lentiviral vectors, and subsequent selection with puromycin (2 μg/ml, Sigma) or G418 (1 mg/ml, Promega) as previously described (Busnadiego et al., 2014). ISG expression was induced in these cell lines using doxycycline hyclate (125 ng/ml, Sigma) for 24 hours prior to viral challenge.

For further examination of the candidate 'directly acting inhibitors' of incoming retroviral infection, human and macaque ISGs that conferred >2-fold protection from HIV-1 or HIV-2 infection in any incoming screen were investigated for their ability to protect cells from incoming HIV. This ISG list was filtered to remove ISGs that activated ISRE/IFNB1 driven reporter expression by >5-fold. The remaining ISGs (Human ISGs AKT3, B2M, BCL3, C5orf39, CCDC109B, CCL2, CCL4, CCL5, CDKN1A, CEBPD, cGAS, DDIT4, DEFB1, EPAS1, FAM46C, FBXO6, HPSE, IDO1, IFI30, IFITM3, IL15, IRF2, LGALS9, MKX, MT1H, Mx2, NOS2A, SCARB2, SP100, TRIM5, TRIM56 and UNC84B in addition to macaque ISGs AKT3, BCL3, BRDG1, BTN3A2, BTN3A2, BUB1, C1orf38, cGAS, CCNA1, CDKN1A, CHMP5, ELF1, GMPR2, IFI16, MDA5, IFITM3, IDO1, LDB1, LGALS9, LY6E, MKX, MT1E , Mx2, NAPA, PAK3, SAMD9, SAT1, SLC16A4, TLR1, TLR3, TLR7, TMEM140, TNFSF13B, TNFSF18, TRIM5-1, TRIM5-2, TRIM5-3, TRIM5-4 and TRIMCYP) were considered further and ISGs that conferred > 2-fold protection in the follow up subscreen are displayed in Fig 3. Human APOBEC3A met the criteria but was not tested in the subscreen due to low transduction levels. Human C5orf39 and NOS2A were overtly toxic in MT4 cells and were not considered further in this context. We were unable to achieve efficient transduction of THP-1 cells using vectors encoding macaque SAT1 and this gene was not considered further in this context.

CRISPR-mediated TRIM56 knockout

A derivative of the HIV based retroviral vector lentiCRISPR Version 2 (Addgene, Plasmid #52961) was constructed by replacing the puromycin resistance gene with a blasticidin resistance gene. TRIM56 CRISPR knockout constructs were made by inserting targeted guide sequences via *Bsm*BI into the modified vector. The CRISPR guide sequences CR1 and CR3 were designed using the CRISPR design program available at http://crispr.mit.edu/ (CR1 targets TRIM56 bp171-191 CGAGTGCCGCGAGACAGTGCC; CR3 targets TRIM56 bp 183-203, CGACAGTGCCTGTGCCGCCCGA). MT4-LTR-GFP knockout cells were derived by transduction with lentiCRISPRV2 based viruses followed by selection with 5μg/ml blasticidin. Single-cell clones derived from populations of cells transduced with control, CR1 and CR3 vectors were derived by limiting dilution and screened for strongly reduced or absent TRIM56 expression by western blotting. None of the control subclones exhibited reduced or absent TRIM56 expression.

Single cycle replication assays

For the incoming, single-cycle infectivity assays in the MT4 cells lines with doxycycline-induced IDO1, TRIM5α, or TagRFP expression and all titration experiments to determine infectious units in MT4 or MT4-LTR-GFP cells, cells were treated or not treated with doxycycline hyclate for 24h before viral challenge. At 16h post-infection, dextran sulfate was added to the HIV-1 (NHG) infected cells to limit infection to a single cycle. Cells were fixed 48h post-infection and the percentage of GFP+ cells determined by flow cytometry.

For viral production assays, MT4 cell lines were treated or untreated for 24h with doxycycline hyclate before infection with HIV-1 (NHG or NL4-3) using a MOI of ~0.3 or HIV-2 (VSV-G pseudotyped ROD10) using an MOI of ~0.6. Cells were also treated with L-tryptophan (Melford) or 1-methyl-L-tryptophan (1-MT, Sigma-Aldrich) at the time of infection, as indicated. At 44h post-infection, cells were lysed in SDS sample buffer and virus-containing

supernatant was harvested and filtered (0.22 um), before being titrated onto MT4 cells, in the case of NHG or TZM-bl cells in the case of HIV-1 NL4-3 and HIV-2.

For single cycle replication assays in A549/TZM-bl cells, cells were seeded in 6-well plates and treated the following day, as indicated, with interferon-gamma (IFNγ, Life Technologies, PHC4031) in the absence or presence of L-tryptophan (50 ug/ml in A549 cells and 33 ug/ml in TZM-bl cells) or 1-MT (100 ug/ml). The unit dose of IFNγ was determined using the most conservative estimate given by the manufacturer ($2x10^6$ units/mg). At 24h after IFNγ treatment, cells were infected with VSV-G pseudotyped NHG for 6h, after which the inoculum was removed, and cells were returned to their original medium (containing IFNγ and 1-MT or L-trp as specified). For the incoming infectivity assay, the A549 cells were harvested and fixed at 44h after infection, and the GFP+ cells were enumerated using flow cytometry. In the outgoing, viral production assay in A549/TZM-bl cells, at 44h post-infection cells were lysed in SDS sample buffer and the virus-containing supernatant was harvested and filtered and titrated onto MT4 cells as described above.

Single cycle infectivity assays conducted using GHOSTX4 and GHOSTX4 TRIM56 cells were executed by infecting cells at an MOI of 0.5 with VSV-pseudotyped HIV-1 NL4-3 or NL-YU2. Incoming virus was removed and replaced with fresh medium 16 hours post infection. Forty-eight hours post-infection the virions were harvested from culture supernatants and cells were lysed in SDS sample buffer.

Spreading viral replication assays

For HIV-1 spreading replication assays in transduced MT4 cells, these cells were doxycycline-treated or untreated for 24h and then were infected with HIV-1 (NHG) at a low MOI of ~0.01. Alternatively, MT4-LTR-GFP cells (and derivatives that were subjected to control or TRIM56 CRISPR knockout) were infected with NL4-3 at an MOI of 0.001 following either no treatment or treatment with 25U/ml IFNα for 24h. Infected GFP+ cells were enumerated every 1-2 days by using flow cytometry.

Spreading replication assays conducted in GHOSTX4-vector and GHOSTX4-TRIM56 clones were performed by infecting cells at an MOI of 0.01 with HIV-1 NL4-3 and derivatives (e.g. HIV-1(TRIM56R)). Every two or three days the cells were split 1 in 5 until cell death terminated the experiment. A portion of the cells was fixed in 2% paraformaldehyde (final concentration) and the level of infection was measured using GFP expression determined through flow cytometry.

Derivation of HIV-1/TRIM5R

To adapt HIV-1 to replicate in GHOSTX4#2 cells, HIV-1/NL4-3 that had been passaged twice in other GHOSTX4-TRIM56 clones was used to infect GHOSTX4 and GHOSTX4-TRIM56#2 cells and virus replication was monitored by enumerating GFP+ cells. When viral spread became evident in GHOSTX4-TRIM56#2 cells (>50% GFP+ cells) viral supernatant from GHOSTX4-TRIM56#2 cells was filtered and used to inoculate fresh cultures of GHOSTX4 and GHOSTX4-TRIM56#2 (MOI=0.01-0.02). After 8 passages in GHOSTX4-TRIM56#2 cells, a full length HIV-1 clone was derived from infected GHOSTX4-TRIM56#2 cells by extracting genomic DNA (Qiagen QIAamp DNA Mini Kit) from the cells when they were 50% GFP positive and amplifying the integrated viral DNA in two portions. The 5'half was amplified using HIV-1 specific primers from the 5'LTR to the *Eco*RI site in *vpr*, the 3' half was amplified using HIV-1 specific primers from the *Eco*RI site in *vpr* to the end of the 3'LTR. The amplified 5' and 3' portions of TRIM56R were then used to generate chimeric proviral plasmids containing portions of HIV-1/NL4-3 and HIV-1/TRIM56R.

Quantitative Western blot analyses

Cell lysates and virions (isolated via centrifugation through 20% sucrose) were resuspended in SDS sample buffer, resolved on NuPage 4-12% Bis-Tris gels (Novex), blotted onto nitrocellulose membranes (GE Healthcare), and probed with either anti-HIV p24 capsid antibody (183-H12-5C, NIH AIDS reagents program), anti-HIV-1 gp120 (American Research Products, 12-6205-1), anti-HIV-1 gp160 (NIH AIDS Reagents Program HIV-1 gp41 Hybridoma Chessie 8), anti-HIV-1 Nef (NIH AIDS Reagents Program, 2949) anti-tubulin (Sigma, T6074), anti-actin (JLA20 hybridoma, Developmental Studies Hybridoma Bank, University of Iowa), anti-c-myc (9E10 hybridoma, Developmental Studies Hybridoma Bank, University of Iowa), anti-TRIM56 (Abcam ab154862) and anti-IDO1 (Abcam, ab55305). Membranes were subsequently probed with secondary, fluorescently labeled goat anti-mouse/anti-rabbit antibodies labeled with IRDye® 800CW or IRDye® 680RD (LI-COR Biosciences or Thermo Scientific) and scanned using a Li-Cor Odyssey Scanner.

Microarray analyses

Total RNA was extracted, using the RNeasy Plus Mini kit (Qiagen), from MT4-LTR-GFP cells control subclones and CRISPR knockout subclones that were untreated or treated with 25 U/ml IFNα (Sigma) for 24 h before harvest.

Supplemental References

Adachi, A., Gendelman, H.E., Koenig, S., Folks, T., Willey, R., Rabson, A., and Martin, M.A. (1986). Production of acquired immunodeficiency syndrome-associated retrovirus in human and nonhuman cells transfected with an infectious molecular clone. Journal of virology *59*, 284-291.

Andrejeva, J., Childs, K.S., Young, D.F., Carlos, T.S., Stock, N., Goodbourn, S., and Randall, R.E. (2004). The V proteins of paramyxoviruses bind the IFN-inducible RNA helicase, mda-5, and inhibit its activation of the IFN-beta promoter. Proceedings of the National Academy of Sciences of the United States of America *101*, 17264-17269.

Berger, G., Durand, S., Fargier, G., Nguyen, X.N., Cordeil, S., Bouaziz, S., Muriaux, D., Darlix, J.L., and Cimarelli, A. (2011). APOBEC3A is a specific inhibitor of the early phases of HIV-1 infection in myeloid cells. PLoS pathogens *7*, e1002221.

Bock, M., Heinkelein, M., Lindemann, D., and Rethwilm, A. (1998). Cells expressing the human foamy virus (HFV) accessory Bet protein are resistant to productive HFV superinfection. Virology *250*, 194-204.

Brass, A.L., Huang, I.C., Benita, Y., John, S.P., Krishnan, M.N., Feeley, E.M., Ryan, B.J., Weyer, J.L., van der Weyden, L., Fikrig, E.*, et al.* (2009). The IFITM proteins mediate cellular resistance to influenza A H1N1 virus, West Nile virus, and dengue virus. Cell *139*, 1243-1254.

Bregnard, C., Zamborlini, A., Leduc, M., Chafey, P., Camoin, L., Saib, A., Benichou, S., Danos, O., and Basmaciogullari, S. (2013). Comparative proteomic analysis of HIV-1 particles reveals a role for Ezrin and EHD4 in the Nef-dependent increase of virus infectivity. Journal of virology *87*, 3729-3740.

Burdette, D.L., Monroe, K.M., Sotelo-Troha, K., Iwig, J.S., Eckert, B., Hyodo, M., Hayakawa, Y., and Vance, R.E. (2011). STING is a direct innate immune sensor of cyclic di-GMP. Nature *478*, 515-518.

Compton, A.A., Bruel, T., Porrot, F., Mallet, A., Sachse, M., Euvrard, M., Liang, C., Casartelli, N., and Schwartz, O. (2014). IFITM proteins incorporated into HIV-1 virions impair viral fusion and spread. Cell host & microbe *16*, 736-747.

Deb, A., Haque, S.J., Mogensen, T., Silverman, R.H., and Williams, B.R. (2001). RNA-dependent protein kinase PKR is required for activation of NF-kappa B by IFN-gamma in a STAT1-independent pathway. Journal of immunology *166*, 6170-6180.

Donahue, D.A., Amraoui, S., di Nunzio, F., Kieffer, C., Porrot, F., Opp, S., Diaz-Griffero, F., Casartelli, N., and Schwartz, O. (2016). SUN2 Overexpression Deforms Nuclear Shape and Inhibits HIV. Journal of virology *90*, 4199-4214.

Furtak, V., Mulky, A., Rawlings, S.A., Kozhaya, L., Lee, K., Kewalramani, V.N., and Unutmaz, D. (2010). Perturbation of the P-body component Mov10 inhibits HIV-1 infectivity. PloS one *5*, e9081.

Gao, D., Wu, J., Wu, Y.T., Du, F., Aroh, C., Yan, N., Sun, L., and Chen, Z.J. (2013). Cyclic GMP-AMP synthase is an innate immune sensor of HIV and other retroviruses. Science *341*, 903-906.

Gao, G., Guo, X., and Goff, S.P. (2002). Inhibition of retroviral RNA production by ZAP, a CCCH-type zinc finger protein. Science *297*, 1703-1706.

Gibbert, K., Francois, S., Sigmund, A.M., Harper, M.S., Barrett, B.S., Kirchning, C.J., Lu, M., Santiago, M.L., and Dittmer, U. (2014). Friend retrovirus drives cytotoxic effectors through Toll-like receptor 3. Retrovirology *11*, 126.

Goujon, C., Moncorge, O., Bauby, H., Doyle, T., Ward, C.C., Schaller, T., Hue, S., Barclay, W.S., Schulz, R., and Malim, M.H. (2013). Human MX2 is an interferon-induced post-entry inhibitor of HIV-1 infection. Nature *502*, 559-562.

Hatziioannou, T., Cowan, S., Goff, S.P., Bieniasz, P.D., and Towers, G.J. (2003). Restriction of multiple divergent retroviruses by Lv1 and Ref1. The EMBO journal *22*, 385-394.

Hishiki, T., Ohshima, T., Ego, T., and Shimotohno, K. (2007). BCL3 acts as a negative regulator of transcription from the human T-cell leukemia virus type 1 long terminal repeat through interactions with TORC3. The Journal of biological chemistry *282*, 28335-28343.

Kane, M., Case, L.K., Wang, C., Yurkovetskiy, L., Dikiy, S., and Golovkina, T.V. (2011). Innate immune sensing of retroviral infection via Toll-like receptor 7 occurs upon viral entry. Immunity *35*, 135-145.

Kemler, I., Barraza, R., and Poeschla, E.M. (2002). Mapping the encapsidation determinants of feline immunodeficiency virus. Journal of virology *76*, 11889-11903.

Kim, Y.M., Brinkmann, M.M., Paquet, M.E., and Ploegh, H.L. (2008). UNC93B1 delivers nucleotide-sensing toll-like receptors to endolysosomes. Nature *452*, 234-238.

Kuang, Z., Seo, E.J., and Leis, J. (2011). Mechanism of inhibition of retrovirus release from cells by interferon-induced gene ISG15. Journal of virology *85*, 7153-7161.

Lahaye, X., Satoh, T., Gentili, M., Cerboni, S., Silvin, A., Conrad, C., Ahmed-Belkacem, A., Rodriguez, E.C., Guichou, J.F., Bosquet, N., *et al.* (2016). Nuclear Envelope Protein SUN2 Promotes Cyclophilin-A-Dependent Steps of HIV Replication. Cell reports.
Lee, Y.N., and Bieniasz, P.D. (2007). Reconstitution of an infectious human endogenous retrovirus. PLoS pathogens *3*, e10.
Leiden, J.M., Wang, C.Y., Petryniak, B., Markovitz, D.M., Nabel, G.J., and Thompson, C.B. (1992). A novel Ets-related transcription factor, Elf-1, binds to human immunodeficiency virus type 2 regulatory elements that are required for inducible trans activation in T cells. Journal of virology *66*, 5890-5897.
Liu, Z., Pan, Q., Ding, S., Qian, J., Xu, F., Zhou, J., Cen, S., Guo, F., and Liang, C. (2013). The interferon-inducible MxB protein inhibits HIV-1 infection. Cell host & microbe *14*, 398-410.
Lu, J., Pan, Q., Rong, L., He, W., Liu, S.L., and Liang, C. (2011). The IFITM proteins inhibit HIV-1 infection. Journal of virology *85*, 2126-2137.
Matsuura, A., Tsukada, J., Mizobe, T., Higashi, T., Mouri, F., Tanikawa, R., Yamauchi, A., Hirashima, M., and Tanaka, Y. (2009). Intracellular galectin-9 activates inflammatory cytokines in monocytes. Genes to cells : devoted to molecular & cellular mechanisms *14*, 511-521.
McLaren, P.J., Gawanbacht, A., Pyndiah, N., Krapp, C., Hotter, D., Kluge, S.F., Gotz, N., Heilmann, J., Mack, K., Sauter, D., *et al.* (2015). Identification of potential HIV restriction factors by combining evolutionary genomic signatures with functional analyses. Retrovirology *12*, 41.
Mitrophanous, K., Yoon, S., Rohll, J., Patil, D., Wilkes, F., Kim, V., Kingsman, S., Kingsman, A., and Mazarakis, N. (1999). Stable gene transfer to the nervous system using a non-primate lentiviral vector. Gene therapy *6*, 1808-1818.
Nakamura, N., Lill, J.R., Phung, Q., Jiang, Z., Bakalarski, C., de Maziere, A., Klumperman, J., Schlatter, M., Delamarre, L., and Mellman, I. (2014). Endosomes are specialized platforms for bacterial sensing and NOD2 signalling. Nature *509*, 240-244.
Neil, S., Martin, F., Ikeda, Y., and Collins, M. (2001). Postentry restriction to human immunodeficiency virus-based vector transduction in human monocytes. Journal of virology *75*, 5448-5456.
Neil, S.J., Zang, T., and Bieniasz, P.D. (2008). Tetherin inhibits retrovirus release and is antagonized by HIV-1 Vpu. Nature *451*, 425-430.
Newman, R.M., Hall, L., Connole, M., Chen, G.L., Sato, S., Yuste, E., Diehl, W., Hunter, E., Kaur, A., Miller, G.M., *et al.* (2006). Balancing selection and the evolution of functional polymorphism in Old World monkey TRIM5alpha. Proceedings of the National Academy of Sciences of the United States of America *103*, 19134-19139.
Nguyen, D.G., Wolff, K.C., Yin, H., Caldwell, J.S., and Kuhen, K.L. (2006). "UnPAKing" human immunodeficiency virus (HIV) replication: using small interfering RNA screening to identify novel cofactors and elucidate the role of group I PAKs in HIV infection. Journal of virology *80*, 130-137.
Pasare, C., and Medzhitov, R. (2005). Toll-like receptors: linking innate and adaptive immunity. Advances in experimental medicine and biology *560*, 11-18.
Pauls, E., Ruiz, A., Riveira-Munoz, E., Permanyer, M., Badia, R., Clotet, B., Keppler, O.T., Ballana, E., and Este, J.A. (2014). p21 regulates the HIV-1 restriction factor SAMHD1. Proceedings of the National Academy of Sciences of the United States of America *111*, E1322-1324.
Perez-Caballero, D., Soll, S.J., and Bieniasz, P.D. (2008). Evidence for restriction of ancient primate gammaretroviruses by APOBEC3 but not TRIM5alpha proteins. PLoS pathogens *4*, e1000181.
Pincetic, A., Kuang, Z., Seo, E.J., and Leis, J. (2010). The interferon-induced gene ISG15 blocks retrovirus release from cells late in the budding process. Journal of virology *84*, 4725-4736.
Randall, R.E., and Goodbourn, S. (2008). Interferons and viruses: an interplay between induction, signalling, antiviral responses and virus countermeasures. The Journal of general virology *89*, 1-47.
Sayah, D.M., Sokolskaja, E., Berthoux, L., and Luban, J. (2004). Cyclophilin A retrotransposition into TRIM5 explains owl monkey resistance to HIV-1. Nature *430*, 569-573.
Schmidt, M., and Rethwilm, A. (1995). Replicating foamy virus-based vectors directing high level expression of foreign genes. Virology *210*, 167-178.
Sheehy, A.M., Gaddis, N.C., Choi, J.D., and Malim, M.H. (2002). Isolation of a human gene that inhibits HIV-1 infection and is suppressed by the viral Vif protein. Nature *418*, 646-650.
Soll, S.J., Neil, S.J., and Bieniasz, P.D. (2010). Identification of a receptor for an extinct virus. Proceedings of the National Academy of Sciences of the United States of America *107*, 19496-19501.
Soneoka, Y., Cannon, P.M., Ramsdale, E.E., Griffiths, J.C., Romano, G., Kingsman, S.M., and Kingsman, A.J. (1995). A transient three-plasmid expression system for the production of high titer retroviral vectors. Nucleic acids research *23*, 628-633.

Stremlau, M., Owens, C.M., Perron, M.J., Kiessling, M., Autissier, P., and Sodroski, J. (2004). The cytoplasmic body component TRIM5alpha restricts HIV-1 infection in Old World monkeys. Nature *427*, 848-853.
Taylor, H.E., Khatua, A.K., and Popik, W. (2014). The innate immune factor apolipoprotein L1 restricts HIV-1 infection. Journal of virology *88*, 592-603.
Telenti, A., and Johnson, W.E. (2012). Host genes important to HIV replication and evolution. Cold Spring Harbor perspectives in medicine *2*, a007203.
Wang, X., Han, Y., Dang, Y., Fu, W., Zhou, T., Ptak, R.G., and Zheng, Y.H. (2010). Moloney leukemia virus 10 (MOV10) protein inhibits retrovirus replication. The Journal of biological chemistry *285*, 14346-14355.
Wiegand, H.L., Doehle, B.P., Bogerd, H.P., and Cullen, B.R. (2004). A second human antiretroviral factor, APOBEC3F, is suppressed by the HIV-1 and HIV-2 Vif proteins. The EMBO journal *23*, 2451-2458.
Wilson, S.J., Schoggins, J.W., Zang, T., Kutluay, S.B., Jouvenet, N., Alim, M.A., Bitzegeio, J., Rice, C.M., and Bieniasz, P.D. (2012). Inhibition of HIV-1 particle assembly by 2',3'-cyclic-nucleotide 3'-phosphodiesterase. Cell host & microbe *12*, 585-597.
Wilson, S.J., Webb, B.L., Ylinen, L.M., Verschoor, E., Heeney, J.L., and Towers, G.J. (2008). Independent evolution of an antiviral TRIMCyp in rhesus macaques. Proceedings of the National Academy of Sciences of the United States of America *105*, 3557-3562.
Xu, H., Yang, J., Gao, W., Li, L., Li, P., Zhang, L., Gong, Y.N., Peng, X., Xi, J.J., Chen, S.*, et al.* (2014). Innate immune sensing of bacterial modifications of Rho GTPases by the Pyrin inflammasome. Nature *513*, 237-241.
Yan, N., Regalado-Magdos, A.D., Stiggelbout, B., Lee-Kirsch, M.A., and Lieberman, J. (2010). The cytosolic exonuclease TREX1 inhibits the innate immune response to human immunodeficiency virus type 1. Nature immunology *11*, 1005-1013.
Yoon, C.H., Kim, S.Y., Byeon, S.E., Jeong, Y., Lee, J., Kim, K.P., Park, J., and Bae, Y.S. (2015). p53-derived host restriction of HIV-1 replication by protein kinase R-mediated Tat phosphorylation and inactivation. Journal of virology *89*, 4262-4280.
Yu, Q., Chen, D., Konig, R., Mariani, R., Unutmaz, D., and Landau, N.R. (2004). APOBEC3B and APOBEC3C are potent inhibitors of simian immunodeficiency virus replication. The Journal of biological chemistry *279*, 53379-53386.
Zennou, V., and Bieniasz, P.D. (2006). Comparative analysis of the antiretroviral activity of APOBEC3G and APOBEC3F from primates. Virology *349*, 31-40.
Zhang, F., Hatziioannou, T., Perez-Caballero, D., Derse, D., and Bieniasz, P.D. (2006). Antiretroviral potential of human tripartite motif-5 and related proteins. Virology *353*, 396-409.